ISSN: 0278-6826 print / 1521-7388 online DOI: 10.1080/02786826.2010.551672



Heterogeneous Atmospheric Chemistry, Ambient Measurements, and Model Calculations of N₂O₅: A Review

Wayne L. Chang,¹ Prakash V. Bhave,² Steven S. Brown,³ Nicole Riemer,⁴ Jochen Stutz,⁵ and Donald Dabdub¹

¹Department of Mechanical and Aerospace Engineering, University of California, Irvine, California, USA

²Atmospheric Modeling and Analysis Division, National Exposure Research Laboratory, USA Environmental Protection Agency, Research Triangle Park, North Carolina, USA

³Earth Systems Research Laboratory, National Oceanic and Atmospheric Administration, Boulder, Colorado, USA

For several decades, dinitrogen pentoxide (N_2O_5) has been recognized as an important reactive intermediate in the atmospheric chemistry of nitrogen oxides and nitrate aerosol, especially during nighttime. However, due to the lack of ambient observations of N_2O_5 , the nocturnal nitrogen oxide chemistry could not be quantified until recent years. The objective of the present article is to assess the current state-of-the-art knowledge of N_2O_5 dynamics within the tropospheric aerosol. An up-to-date summary of N_2O_5 chemistry and major loss mechanisms are provided. Furthermore, techniques for measuring ambient N_2O_5 and an overview of typical N_2O_5 levels in the troposphere are described. In addition, model representations of N_2O_5 chemistry are reviewed along with key features of N_2O_5 vertical profiles based on numerical simulations. Lastly, the article provides the outstanding uncertainties and needs for further research into the atmospheric chemistry of N_2O_5 . These

Received 30 June 2010; accepted 30 December 2010.

This review article was motivated by a series of presentations at the 2007 International Aerosol Modeling Algorithms conference in Davis, California. We are appreciative of funding from the California Air Resource Board (ARB) and grateful to Dr. Ajith Kaduwala for his support. The United States Environmental Protection Agency (US EPA) through its Office of Research and Development collaborated in the research described here. It has been subjected to Agency review and approved for publication. We also thank Susan Forbes (US EPA) for her assistance with literature searches, and William R. Simpson, Randy Apodaca, Timothy Bertram, and Ezra Wood for providing several figures. Furthermore, we extend our thanks to the reviewers for their invaluable constructive comments and suggestions that have truly improved the quality of this work.

Address correspondence to Donald Dabdub, Department of Mechanical and Aerospace Engineering, University of California, 4226 Engineering Gateway, Irvine, CA 92697, USA. E-mail: ddabdub@uci.edu

include the need for better characterization of N_2O_5 heterogeneous uptake under temperature conditions characteristic of mid- and high-latitude winter seasons; greater understanding of the influence of individual aerosol components on N_2O_5 uptake and representation of these components in atmospheric models; and comprehensive descriptions of nighttime vertical profiles of N_2O_5 and related pollutants.

1. INTRODUCTION

Dinitrogen pentoxide (N_2O_5) is an important reactive intermediate in the atmospheric chemistry of nitrogen oxides. It was first recognized as a limiting factor in the destruction of ozone (O_3) by NO and NO₂ in the lower stratosphere (Johnston 1971; Crutzen 1971). In the troposphere, N_2O_5 has long been understood to be a sink for NO_x (NO_x = NO + NO₂) through its reaction with water (either in the gas or particle phase) to produce HNO₃, which has a direct effect on tropospheric ozone production (Morris and Niki 1973; Mozurkewich and Calvert 1988) and particulate matter (PM) formation (Russell and Cass 1986). Although the formation and loss of N_2O_5 is generalized in kinetic mechanisms for photochemical smog (Hecht and Seinfeld 1972; Atkinson et al. 2004), its significance has been open to question for several decades (Calvert 1976; Brown et al. 2006b).

The lifetime of NO_x , a key player in atmospheric chemistry, depends critically on the overnight fate of N_2O_5 , which may either serve as a reservoir that allows for reversible storage and transport or as a sink that leads to efficient overnight removal of NO_x (Dentener and Crutzen 1993). During the night, N_2O_5 is in rapid equilibrium with the nitrate radical, NO_3 , one of the main nocturnal atmospheric oxidants (Wayne et al. 1991).

 $^{^4}$ Department of Atmospheric Sciences, University of Illinois at Urbana-Campaign, Urbana, Illinois, USA

⁵Department of Atmospheric and Oceanic Sciences, University of California, Los Angeles, California, USA

A determining factor of NO_3 availability, and thus nighttime oxidative capacity, is the hydrolysis of N_2O_5 , which, depending on its efficiency, may consume a large fraction of the NO_3 produced at night. The gas-phase reaction of N_2O_5 with H_2O is slow and relatively constant, while the heterogeneous reaction is more variable and can be quite rapid on particle surfaces (Mozurkewich and Calvert 1988; Li et al. 1993; Patris et al. 2007). The overnight removal of NO_3 and N_2O_5 directly impacts the production of oxidants such as hydroxyl radical (OH) and ozone at dawn. The resulting impacts on regional O_3 are complex. Due to the nonlinear relationship between NO_x concentration and ozone production, heterogeneous hydrolysis of N_2O_5 is predicted to decrease ozone under low- NO_x conditions and increase ozone in high- NO_x regions (Riemer et al. 2003).

Several air quality modeling studies have demonstrated the influence of tropospheric N₂O₅ on oxidant levels at the urban (Russell et al. 1985; Lei et al. 2004), regional (Riemer et al. 2003; McLaren et al. 2004), and global scales (Dentener and Crutzen 1993: Tie et al. 2001, 2003: Evans and Jacob 2005: Feng and Penner 2007). The tropospheric aerosol budget is also directly influenced by N₂O₅ because its main hydrolysis product, nitric acid, partitions favorably to the aerosol phase at low temperatures or in environments with excess ammonia (Stelson and Seinfeld 1982; Russell and Cass 1986). Direct N₂O₅ uptake by particles and fog droplets is also an important source of dissolved nitrate (Lillis et al. 1999). Particle-phase nitrate dynamics is still a major area of uncertainty in atmospheric aerosol prediction today (Yu et al. 2005) and has significant impacts on regional air quality and climate (Liao and Seinfeld 2005; Feng and Penner 2007; Bauer et al. 2007).

Despite its importance, many aspects of tropospheric N_2O_5 chemistry are still not well known. The rate of N_2O_5 uptake by particles, which depends on aerosol composition and meteorological conditions (relative humidity (RH) and temperature), remains highly uncertain (Brown et al. 2006b; Bertram et al. 2009). Only recently, the heterogeneous chemistry of N_2O_5 on chloride-containing aerosol, known from laboratory studies for two decades (Finlayson-Pitts et al. 1989a), has been shown to efficiently release atomic chlorine radicals to the atmosphere (Osthoff et al. 2008). The impacts of this chemistry on regional and global scales are still unknown. In addition, little is known about the vertical distribution of N_2O_5 in the nocturnal atmosphere. Many of these questions can be answered by novel atmospheric measurement techniques that have emerged only recently.

We provide an overview of the current knowledge of N_2O_5 chemistry in the troposphere and identify the most pressing research needs. After summarizing the known N_2O_5 chemistry and the dominant loss pathways in Section 2, Section 3 describes the ambient N_2O_5 measurement techniques that are currently available. Section 4 presents a discussion of the key observations of ambient N_2O_5 , including typical concentrations and vertical distributions during nighttime. Section 5 outlines the representation of N_2O_5 chemistry in atmospheric models, tro-

pospheric N_2O_5 vertical gradients based on simulation results, and related challenges facing the modeling community. Finally, Section 6 presents our conclusions and identifies areas where further research is needed most urgently.

2. ATMOSPHERIC N₂O₅ CHEMISTRY

 N_2O_5 is formed from the gas-phase oxidation of NO_2 by O_3 , followed by the reaction of NO_2 with NO_3 (R1 and R2a):

$$NO_2 + O_3 \rightarrow NO_3 + O_2,$$
 [R1]

$$NO_3 + NO_2 \rightarrow N_2O_5$$
, [R2a]

$$N_2O_5 \rightarrow NO_3 + NO_2$$
. [R2b]

 N_2O_5 is thermally unstable, so it dissociates back to NO_3 and NO_2 [Reaction (R2b)]. The equilibrium between NO_2 , NO_3 , and N_2O_5 is given by

$$[N_2O_5] = K_{eq}[NO_2][NO_3],$$
 [1]

where K_{eq} is a temperature-dependent equilibrium constant (cm³ molecule $^{-1}$). Cool weather promotes a shift in the equilibrium of Reaction (R2) toward N_2O_5 , as shown in Figure 1. Whereas N_2O_5 and NO_3 are in roughly equal proportions at 1 ppbv NO_2 and 295 K, the ratio of N_2O_5 to NO_3 is approximately 10 at 278 K. In addition, N_2O_5 typically exceeds NO_3 under polluted conditions (e.g., 10 ppbv NO_2).

Two different loss pathways have to be considered for N_2O_5 : direct losses, in which N_2O_5 undergoes hydrolysis reactions, and

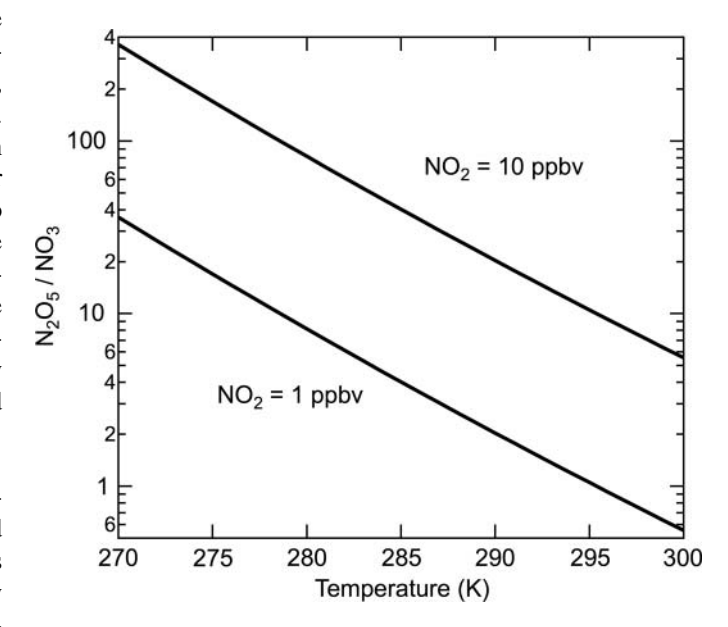


FIG. 1. The N_2O_5/NO_3 ratio as a function of temperature using $K_{\rm eq} = A \cdot \exp(B/T)$, in which T is the temperature in Kelvin, $A = 2.7 \times 10^{-27} \, {\rm cm}^3$ molecule⁻¹, and B = 11,000 (Sander et al. 2006). Other recommendations for $K_{\rm eq}$ are in close agreement with this expression (Osthoff et al. 2007).

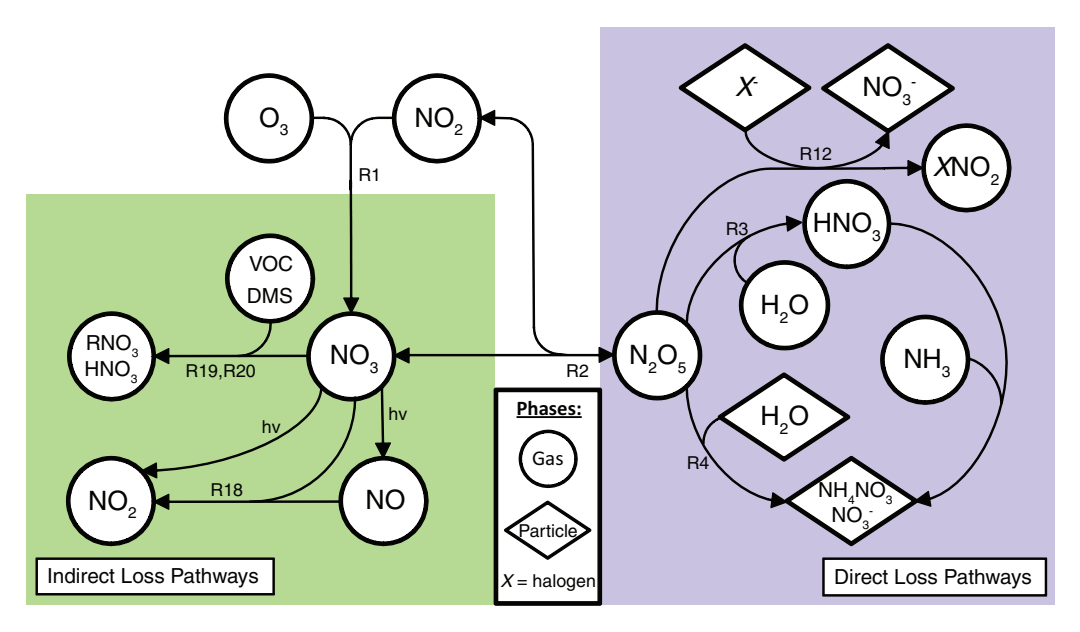


FIG. 2. Chemical mechanism for N_2O_5 formation and loss. X indicates halogen atoms such as chlorine and bromine that are commonly found in sea-salt aerosol. Circles denote gas-phase species, and diamonds denote species in particle phase. (Figure provided in color online.)

indirect pathways, in which a loss of NO_3 or NO_2 propagates through thermal equilibrium and thus leads to an N_2O_5 decrease. The relative importance of these two pathways is determined by the temperature-dependent equilibrium [Equation (1)] and the presence of various reactants of NO_3 , NO_2 , and N_2O_5 (including uptake on surfaces). A schematic of the major loss pathways is shown in Figure 2.

2.1. Direct Loss Pathways

The direct chemical loss of atmospheric N_2O_5 proceeds through its hydrolysis reaction (Morris and Niki 1973),

$$N_2O_5(g) + H_2O(g) \rightarrow 2HNO_3(g)$$
. [R3]

It is clear today that this reaction is too slow as a second-order process in the gas phase to have significant impact on the lifetime of N_2O_5 and NO_x (Detener and Crutzen 1993). Wahner and coworkers also reported a moderate contribution of Reaction (R3) to the overall hydrolysis rate but suggested that the third-order reaction, $N_2O_5(g) + 2H_2O(g)$, may be important (Mentel et al. 1996; Wahner et al. 1998a). While Voegele et al. (2003) provide some theoretical insights into the reaction of N_2O_5 with water, further studies of this reaction are still warranted in order to elucidate the magnitude of its potential impact (Section 4.3). Due to the lack of agreement between data obtained from laboratory and field measurement studies, IUPAC (2010) recommend an upper limit of 1×10^{-22} cm³ molecule⁻¹ s⁻¹ for the bimolecular process only, until further insights are obtained.

The heterogeneous hydrolysis of N_2O_5 on and within aerosol particles, fog, or cloud droplets,

$$N_2O_5(g) + H_2O(1) \rightarrow 2HNO_3(aq),$$
 [R4]

has been shown to be much faster than homogeneous hydrolysis under typical tropospheric conditions and is now believed to be the dominant pathway for direct N_2O_5 removal (Russell et al. 1985; Dentener and Crutzen 1993; Hanway and Tao 1998). This reaction can be modeled as a pseudo-first-order process (Heikes and Thompson 1983; Chang et al. 1987):

$$\frac{d[N_2O_5]}{dt}\bigg|_{het} = -k_{N_2O_5}[N_2O_5],$$
 [2]

where dt denotes the time increment and kN_2O_5 represents the rate constant for the heterogeneous surface reaction (Schwartz 1986),

$$k_{\rm N_2O_5} = \left(\frac{r}{D_{\rm g}} + \frac{4}{c_{\rm N_2O_5}\gamma_{\rm N_2O_5}}\right)^{-1} S.$$
 [3]

Here, r is the mean particle radius, $D_{\rm g}$ is the gas-phase diffusion coefficient for N₂O₅, $c_{\rm N_2O_5}$ is the mean molecular velocity of N₂O₅, S is the aerosol surface area density, and $\gamma_{\rm N_2O_5}$ is the reaction probability. Dentener and Crutzen (1993) showed that when $\gamma_{\rm N_2O_5} < 0.1$, the dominant term in Equation (3) is $4/(c_{\rm N_2O_5})$, so the reaction rate constant simplifies to (Riemer et al. 2003):

$$k_{N_2O_5} = \frac{1}{4}c_{N_2O_5} \cdot \gamma_{N_2O_5} \cdot S.$$
 [4]

The reaction probability, $\gamma_{N_2O_5}$, is the fraction of collisions between gaseous N_2O_5 molecules and particle surfaces that result in a loss of N_2O_5 . In other words, it is the likelihood of N_2O_5 uptake on particles. This parameter has been measured under controlled laboratory conditions on three major types of substrates: ice surfaces, water droplets, and aerosol surfaces. The studies on ice surfaces are of critical importance at high latitudes and in the stratosphere (Tolbert et al. 1988; Horn et al. 1994; Apodaca et al. 2008), whereas the studies on water droplets are thought to be important under foggy conditions (Wood et al. 2005; Sommariva et al. 2009) and in clouds. Laboratory measurements on those substrates are summarized by Sander et al. (2006) and are beyond the scope of this review.

Laboratory measurements on aerosol surfaces commonly found in the troposphere show that $\gamma_{N_2O_5}$ is affected by particle composition, RH, and, to a lesser extent, temperature. Most of the early laboratory studies focused on inorganic particle compositions. Davis et al. (2008) reviewed data from seven laboratory studies (Mozurkewich and Calvert 1988: Hu and Abbatt 1997; Folkers 2001; Kane et al. 2001; Folkers et al. 2003; Hallquist et al. 2003; Badger et al. 2006), in which $\gamma_{N_2O_5}$ was measured on ammoniated sulfate and nitrate particles in both crystalline- and aqueous-phase states. Values of $\gamma_{N_2O_5}$ on the aqueous particles range from 0.001 at 29% RH to 0.086 at 76% RH, whereas the values on crystalline particles fall between 0.0003 and 0.012. More recent measurements reported by Bertram and Thornton (2009) and Griffiths and Cox (2009) also fall within these ranges. Heterogeneous uptake of N₂O₅ on sodium-containing particles has also received significant attention because sea-salt surfaces can be a sink for nitrogen oxides and a source of halogen radicals [Reaction (R12)]. Values of $\gamma_{N_2O_5}$ on aqueous NaCl and natural sea-salt particles range from 0.006 at 30% RH to 0.04 at 77% RH (Behnke et al. 1997; Schweitzer et al. 1998; Stewart et al. 2004; Thornton and Abbatt 2005; McNeill et al. 2006). On aqueous NaHSO₄ and Na₂SO₄ particles, $\gamma_{N_2O_5}$ lies at the upper end of that range, between 0.018 and 0.04 (Mentel et al. 1999). In contrast, $\gamma_{N_2O_5}$ on aqueous NaNO₃ particles is more than an order of magnitude lower, falling between 0.0003 and 0.003 (Wahner et al. 1998b; Hallquist et al. 2003). Mentel et al. (1999) proposed a mechanism to explain the suppression of $\gamma_{N_2O_5}$ by nitrate, which has been extended recently by Griffiths et al. (2009).

Several attempts have been made to unify these laboratory observations in a single chemical mechanism. Mozurkewich and Calvert (1988) proposed an N_2O_5 reaction mechanism, which is consistent with the sensitivities of $\gamma_{N_2O_5}$ to RH and aerosol sulfate: N_2O_5 dissolves in water, dissociates to NO_2^+ and NO_3^- , both of which will react with water and H^+ to form HNO_3 .

$$N_2O_5(g) \leftrightarrow N_2O_5(aq),$$
 [R5]

$$N_2O_5(aq) \to NO_3^-(aq) + NO_2^+(aq),$$
 [R6]

$$NO_2^+(aq) + H_2O(1) \rightarrow H^+(aq) + HNO_3(aq),$$
 [R7]

$$NO_3^-(aq) + H^+(aq) \leftrightarrow HNO_3(aq),$$
 [R8]

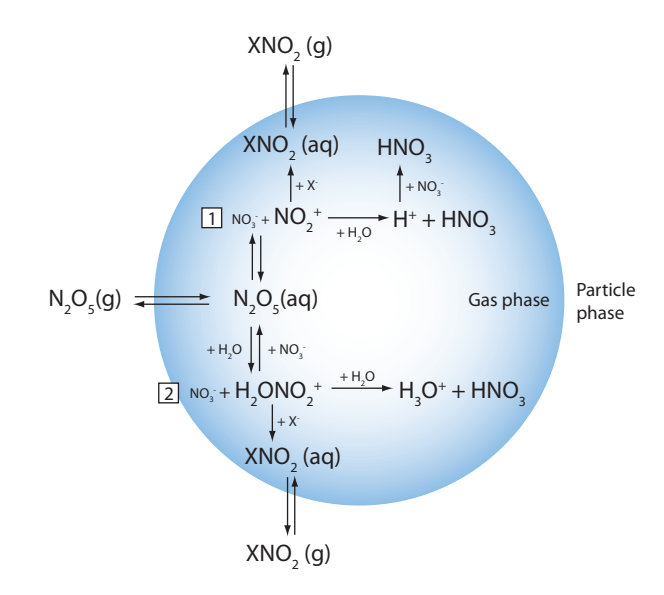


FIG. 3. Schematic depiction of the heterogeneous reaction of N_2O_5 with aqueous particle proposed by Griffiths et al. (2009) in summary of previous studies and Bertram and Thornton (2009). X denotes a halogen species such as chlorine, bromine, and iodine. (Figure provided in color online.)

$$HNO_3(aq) \leftrightarrow HNO_3(g)$$
. [R9]

This "ionic hydrolysis mechanism" was also supported by other authors, e.g., Wahner et al. (1998b), Mentel et al. (1999), Hallquist et al. (2003), and Griffiths et al. (2009). Wahner et al. (1998) explained the lower $\gamma_{N_2O_5}$ for nitrate-containing aerosol by the fact that the recombination reaction $NO_2^+ + NO_3^-$ is favored when large nitrate concentrations are present. Thornton et al. (2003) introduced a modified mechanism for dilute acidic or neutral nonhalide aerosol (Figure 3), which is also consistent with observations of the inhibition of N_2O_5 uptake by aerosol nitrate and the formation of halogen nitrites from aqueous sodium halide aerosol [see (R12) below and related discussion]. In this mechanism, Reactions (R6–R8) of the Mozurkewich mechanisms are replaced by

$$N_2O_5(aq) + H_2O(l) \leftrightarrow [H_2ONO_2^+(aq) + NO_3^-(aq)]^*,$$
[R10]

$$\begin{split} &[H_2ONO_2^+(aq) + NO_3^-(aq)]^* + H_2O(l) \\ &\to HNO_3(aq) + NO_3^-(aq) + H_3O^+. \end{split} \quad [R11]$$

This mechanism involves the formation of the hydrated NO_2^+ intermediate, $H_2ONO_2^+$, instead of NO_2^+ . However, Thornton et al. (2003) and Bertram and Thornton (2009) pointed out that $H_2ONO_2^+$ has thus far never been directly observed in the systems discussed here. On the basis of their results, Bertram and Thornton (2009) developed a parameterization for $\gamma_{N_2O_5}$ as a function of the molar ratios of $H_2O(l)$ to NO_3^- and Cl^- to NO_3^-

for the use in regional and global models (see Section 5.1 for a discussion of model parameterizations of N_2O_5 hydrolysis).

Mozurkewich and Calvert (1988) argued that the diffusion of N₂O₅ into the drop [Reaction (R5)] was expected to be much slower compared to its dissociation [Reaction (R6)] and therefore concluded that the reaction takes place almost entirely in a thin layer near the surface. Hence, the loss of N₂O₅ should be proportional to the aerosol surface area. Thornton et al. (2003) revisited the question of surface versus volume reaction with inconclusive results. According to Mozurkewich and Calvert (1988), the mechanisms (R6)–(R9) are consistent with reaction probabilities becoming smaller at low humidities because under these conditions only a thin layer of liquid may be available. They argued that when this layer is thin enough, N₂O₅ can diffuse uniformly throughout and hence saturate it. As a result, the rate of reevaporation becomes faster. Similarly, the decrease of $\gamma_{N_2O_5}$ with increasing temperature is also consistent with the increase in the rate of evaporation compared to the rate of dissociation.

The mechanism by Bertram and Thornton (2009) also explains the formation of nitryl halide molecules, which was previously observed by Finlayson-Pitts et al. (1989a, b) and Barnes et al. (1991). This reaction is often summarized by

$$N_2O_5(g) + X^-(aq) \to XNO_2(g) + NO_3^-(aq),$$
 [R12]

where X denotes a halogen species such as chlorine, bromine, and iodine. In the case of chlorine, the Bertram and Thornton mechanism and Reaction (R12) indicate that the yield of ClNO₂ depends on the Cl⁻ concentration within the particle, but observed mixing ratios of ClNO₂ in the marine boundary layer as well as mid-continental areas are much higher than predictions made based on ambient particulate chlorine level (Osthoff et al. 2008; Thornton et al. 2010). Another proposed mechanism for the ambient production of ClNO2 is the reaction between gaseous HCl and the autoionized intermediate of N₂O₅, NO₂+NO₃⁻, on water-containing surfaces (Raff et al. 2009). The product distribution from Reaction (R12) as a function of Cl⁻ concentration based on field measurements has been investigated in detail and is discussed further in Section 4.4. The subsequent photolysis of nitryl halides produces halogen radicals (Leu et al. 1995), which can increase the oxidative capacity of the atmosphere, thereby impacting ozone and other gaseous pollutants (Simon et al. 2009). When Reaction (R12) takes place on highly acidic particles, the reaction of N₂O₅ with chloride may even produce Cl2 (Roberts et al. 2008, 2009), which photolyzes rapidly to form two atomic chlorine radicals.

Several studies investigated the uptake of N_2O_5 on mineral dust particles (Seisel et al. 2005; Karagulian et al. 2006; Wagner et al. 2008, 2009). On these substrates, $\gamma_{N_2O_5}$ ranges from 0.005 to 0.3. Seisel et al. (2005) proposed two reaction mechanisms of N_2O_5 on dust. The first reaction proceeds via the reaction of gas-phase N_2O_5 with a surface OH group to form surface nitrate and nitric acid. HNO₃(ads) is assumed to readily react

via Reaction (R15) forming another surface nitrate:

$$N_2O_5(g) + S-OH \to N_2O_5^*S-OH,$$
 [R13]

$$N_2O_5^*S-OH \rightarrow HNO_3(ads) + S-NO_3$$
, [R14]

$$HNO_3(ads) + S-OH \rightarrow H_2O(ads) + S-NO_3,$$
 [R15]

and S is surface site. A second pathway proceeds via the hydrolysis of N_2O_5 , most likely in the interlamellar water of clay minerals in mineral dust (Seisel et al. 2005):

$$N_2O_5(g) + H_2O(ads) \rightarrow 2HNO_3(ads),$$
 [R16]

$$HNO_3(ads) + H_2O(ads) \rightarrow H_3O^+ + NO_3^-$$
. [R17]

Sander et al. (2006) summarized the available measurements of $\gamma_{N_2O_5}$ on soot particles, which vary broadly from 0.0002 to 0.02 at ambient RH. Results from a more recent study on decane flame soot fall within the 0.005–0.03 range (Karagulian and Rossi 2007).

The NO₂⁺-NO₃⁻ intermediate is also recognized as an important source of nitration for organic species in the condensed phase, such as the occurrence of nitrophenols (Harrison et al. 2005). Laboratory measurements of $\gamma_{N_2O_5}$ on organic particles fall into three categories: pure organic particles, mixed organic/inorganic particles, and inorganic particles coated with organic material. The data on pure organic substrates are limited to five studies (Thornton et al. 2003; Badger et al. 2006; Gross and Bertram 2008; Griffiths et al. 2009; Gross et al. 2009). Most of these studies reported $\gamma_{N_2O_5}$ values at least an order of magnitude lower than those measured on aqueous inorganic salts (e.g., 6×10^{-5} on liquid-phase oleic acid and $4-8 \times 10^{-4}$ on liquidphase glycerol). The highest reported values are 0.017–0.03 on malonic acid at 50%-70% RH (Thornton et al. 2003; Griffiths et al. 2009). As in the case of inorganic substrates, several studies have reported $\gamma_{N_2O_5}$ values on solid-phase organics to be much smaller than those on liquid-phase organics (Thornton et al. 2003; Griffiths et al. 2009; Gross et al. 2009). In addition, uptake on solid polycyclic aromatic hydrocarbons was too slow to be measured (Gross and Bertram 2008). Two laboratory studies have explored $\gamma_{N_2O_5}$ on mixed organic/inorganic particles. When humic acid is mixed with increasing amounts of ammonium sulfate ranging from 60% to 94% of the particle mass, $\gamma_{N_2O_5}$ increases from 0.0003 to 0.0083 (Badger et al. 2006). Griffiths et al. (2009) found that the addition of dicarboxylic acids to ammonium bisulfate has a small effect on $\gamma_{N_2O_5}$, but their effect on uptake by ammonium sulfate particles is more pronounced; small amounts of organic acid enhance $\gamma_{N_2O_5}$, while larger amounts inhibit. Numerous laboratory investigations into the effect of organic coatings on $\gamma_{N_2O_5}$ have been reported in recent years (Folkers et al. 2003; Thornton and Abbatt 2005; Anttila et al. 2006; McNeill et al. 2006; Park et al. 2007; Cosman et al. 2008; Cosman and Bertram 2008). Overall, these studies indicate that organic coatings can decrease N₂O₅ uptake coefficients by an order of magnitude or

more. Various explanations for the reduction of $\gamma_{N_2O_5}$ in the presence of organic films have been proposed. Folkers et al. (2003) concluded that the main cause for the decrease of $\gamma_{N_2O_5}$ in the presence of multilayer organic films is a smaller Henry's law constant or mass accommodation coefficient for the films, leading to a slower initial solvation of N₂O₅ in the droplets. Thornton and Abbatt (2005), working with a coating thickness of only a monolayer, proposed a reduction in the accommodation coefficient and the reaction rate at the interface as a possible explanation. Anttila et al. (2006), on the other hand, attributed the decrease of $\gamma_{N_2O_5}$ to the fact that the reaction rate constant of N₂O₅ in the coating is decreased by 3–5 orders of magnitude and that the product of the solubility of N_2O_5 and its diffusion coefficient in the coating are reduced by more than an order of magnitude compared to the corresponding value for the aqueous phase.

With the recent development of in situ techniques for N_2O_5 measurement (Sections 3.2–3.5), it has become possible to determine $\gamma_{N_2O_5}$ on atmospheric aerosol particles, which exhibit more complex chemical composition than those studied in the laboratory setting (Section 4.3). In addition, efforts have been made to incorporate the growing body of $\gamma_{N_2O_5}$ measurements into a unified model parameterization (Section 5.1).

2.2. Indirect Loss Pathways

As noted above, indirect loss of N_2O_5 can proceed through the reactive losses of NO_3 . One of the dominant NO_3 loss pathways during the day and at the surface at night is the reaction with NO (Wayne et al. 1991; Asaf et al. 2010):

$$NO_3 + NO \rightarrow 2NO_2$$
. [R18]

Together with the daytime photolysis of NO_3 (Johnston et al. 1996), Reaction (R18) leads to low daytime concentrations of NO_3 and N_2O_5 . However, under polluted urban conditions, small but nonnegligible concentrations of gas-phase NO_3 and N_2O_5 can be sustained in the daytime (Geyer et al. 2003; Brown et al. 2005; Osthoff et al. 2006). Other major NO_3 loss pathways include reaction with dimethyl sulfide (DMS) and hydrocarbons (Allan et al. 2000), as well as heterogeneous uptake (Moise et al. 2002; Karagulian and Rossi 2007; Gross et al. 2009). The NO_3 reaction with DMS,

$$NO_3 + CH_3SCH_3 \rightarrow CH_3SCH_2 + HNO_3$$
, [R19]

is most important in marine environments (Allan et al. 1999). The reaction with hydrocarbons may also initiate with the abstraction of hydrogen, but with species such as isoprene and terpenes in particular, the reaction is predominately via addition to the carbon–carbon double bond,

$$NO_3 + R-C = C-R' \rightarrow R-C-C(NO_3)-R'$$
. [R20]

Heterogeneous NO₃ reaction rates with aerosols vary with particle compositions and meteorological conditions, analogues to the previously summarized heterogeneous uptake of N₂O₅. While the uptake coefficient of NO₃ on mineral dust is similar in magnitude to the values for N₂O₅, uptake on organics favors NO₃ over N₂O₅ (Tang et al. 2010). Karagulian and Rossi (2005) reported γ_{NO3} values on mineral dusts ranging between 0.034 and 0.12. For soot particles, measured peak γ_{NO3} values vary from 0.0003 to 0.05 (Saathoff et al. 2001; Mak et al. 2007; Karagulian and Rossi 2007). For organic-containing species, 10^{-3} was proposed to be the upper limit of the NO₃ reactive uptake coefficient (McNeill et al. 2007) and 0.015 for liquid and frozen organics (Moise et al. 2002). However, more recent measurements demonstrated much larger uptake coefficient values on organic aerosols. Reported γ_{NO3} values include 0.059-0.79 for polycyclic aromatic hydrocarbons (Gross and Bertram 2008), 0.034 for terminal alkene monolayer (Gross and Bertram 2009), and 0.076–0.62 for liquid alkenoic acids (Gross et al. 2009).

2.3. Overall Nighttime NO_x Loss

Whether through direct or indirect pathways, the loss of N₂O₅ is a controlling factor in the nighttime lifetime of NO_x . Although Reaction (R1) is slow, it is fast enough that it converts a large fraction of the NO_x available at sunset within a given air mass into NO₃. If N₂O₅ hydrolysis is rapid (i.e., first-order rate coefficient larger than $2.5 \times 10^{-4} \text{ s}^{-1}$, corresponding to an uptake coefficient, $\gamma = 0.02$, and an aerosol surface area >200 μ m² cm⁻³), it effectively doubles the rate coefficient for this conversion since Reaction (R1) becomes rate limiting and each NO₃ radical produced goes on to react with a second NO₂ via Reaction (R2a) with very little dissociation [Reaction (R2b)]. For example, during summertime conditions (i.e., 298 K) with a nominal (constant) background of 50 ppbv O₃, the reaction sequence would convert 94% of NO_x to HNO₃ (or HNO₃ + XNO₂) in a 10-h night when estimated with a model; in winter (i.e., 273 K), Reaction (R1) is much slower, but NO_x conversion is still 87% in a 14-h night. If, on the other hand, N₂O₅ hydrolysis is slow, indirect losses via oxidative chemistry Reactions (R19) and (R20) dominate. Predicted summer and winter overnight NO_x loss would be 76% and 64%, respectively, assuming that all NO₃ reactions led to products other than NO₂. In the section on "Field Determinations of the N₂O₅ Uptake Rate," these rates of overnight NO_x loss will be estimated from a review of ambient measurements.

As N_2O_5 and NO_3 are always present in the same air mass, both direct and indirect losses have to be considered for a full picture of N_2O_5 chemistry. Thus, many of the instruments described in the third section, as well as the observations exemplified in the fourth section, measure and determine both tropospheric N_2O_5 and NO_3 levels at the same time.

TABLE 1 Summary of ambient N₂O₅ measurement techniques

	•	2 0		
Technique	Reference	Sensitivity	Averaging time (s)	Field deployment
Equilibrium calculation f	rom measured NO ₂ and NO ₃			
DOAS	Atkinson et al. (1986) Platt and Stutz (2008)	NO ₃ : 2 pptv ^a	5 ^c	Phoenix, Arizona ^b TexAQS ^b
CE-DOAS	Meinen et al. (2010)	NO ₃ : 6.3 pptv ^a	0.001^{c}	N/A
Thermal conversion to N	O_3			
Pulsed CRDS	Brown et al. (2002) Dubé et al. (2006)	N ₂ O ₅ : 1 pptv	1	Boulder, Colorado NEAQS-ITCT 2004, TexAQS II
	Nakayama et al. (2008)	N ₂ O ₅ : 2.2 pptv	100	Toyokawa, Japan
Cw CRDS	Ayers and Simpson (2006)	N_2O_5 : 2 pptv	25	Fairbanks, Alaska
OA CRDS	Ayers et al. (2005)	NO ₃ : 1.4 pptv ^a	4.6	Fairbanks, Alaska
	Crowley et al. (2010)	N_2O_5 : 4 pptv	3	Kleiner Feldberg, Germany
Broadband CRDS	Ball et al. (2001) Bitter et al. (2005)	NO ₃ : 1 pptv ^a	100	NAMBLEX
CEAS	Langridge et al. (2008)	NO ₃ : 0.25 pptv ^a	10	RHaMBLe
	Varma et al. (2009)	NO ₃ : 2 pptv ^a	5	N/A
LIF	Wood et al. (2003) Matsumoto et al. (2005a)	N_2O_5 : 6 pptv	600	Leuschner, California Tokyo, Japan
TD-CIMS	Slusher et al. (2004)	N_2O_5 : 12 pptv	1	Boulder, Colorado
Direct ionization and dete	ection of N ₂ O ₅			
ID-CIMS	Zheng et al. (2008)	N_2O_5 : 30 pptv	10	MCMA-2006/MILAGRO
UW-CIMS	Kercher et al. (2009)	N_2O_5 : 11 pptv	1	ICEALOT 2008

^aSee "Differential Optical Absorption Spectroscopy (DOAS)" section for conversion of NO₃ sensitivity to N₂O₅ sensitivity.

3. TECHNIQUES FOR MEASURING ATMOSPHERIC N_2O_5

There are three schemes for quantifying ambient N_2O_5 . The first is the indirect calculation of N₂O₅ levels on the basis of its equilibrium with two directly measured species, NO₃ and NO₂. This method is common for open-path optical methods. In a closed-cell system, N₂O₅ can be measured by thermal conversion to NO₃ using a heated inlet and subsequent detection of the NO₃ molecules. This is common to in situ optical methods that are highly sensitive to NO₃, as well as to some massspectrometric instruments. These methods invariably measure the sum of NO₃ and N₂O₅, such that differentiation between the two must be accomplished either by a second measurement channel that does not include a thermal converter (thereby providing a measure of NO₃ alone) or by collocation of an NO₂ measurement such that the individual concentrations can be calculated from equilibrium. Finally, N₂O₅ may itself be directly ionized and detected via mass spectrometry. By exploiting these three basic schemes, several analytical techniques have been developed to quantify ambient N₂O₅. The techniques are described in this section and summarized in Table 1.

Many of the optical techniques described in this section have been intercompared during a recent measurement campaign at the SAPHIR environmental simulation chamber in Jülich, Germany (Fry et al. 2008; Rollins et al. 2009; Fuchs et al. 2010). Further description of those instruments and their accuracy will be given in a forthcoming publication (Apodaca et al. 2011). The chemical ionization techniques, however, did not participate in that campaign; consequently, Section 3.5 includes ambient intercomparisons of two chemical ionization instruments with a cavity ring-down spectrometer. Although a few other instrument intercomparisons have been conducted in ambient settings, a full description of them is beyond the scope of this review.

3.1. Differential Optical Absorption Spectroscopy (DOAS)

The first determinations of ambient N_2O_5 were made using long-path DOAS measurements of NO_2 and NO_3 in combination with Equation (1) (Platt et al. 1980; Atkinson et al. 1986). DOAS is a widely recognized detection technique for NO_3 in both remote and highly polluted environments. The advantage of DOAS lies in its ability to measure gaseous species such as

^bVertical profile field deployment measurements.

^cPath lengths (km) are shown instead of the averaging times here.

NO₂ and NO₃ without artifacts associated with wall losses and inlets. Since DOAS does not require calibration, it is considered an absolute analytical technique (Wang et al. 2006). During winter season though, the utility of DOAS for estimating N_2O_5 becomes quite limited by the low NO₃ levels. DOAS has been used to obtain long-term measurements of ground-level NO₃ (and NO₂) at several locations in Europe (e.g., Heintz et al. 1996; Allan et al. 1999; Geyer et al. 2001; Vrekoussis et al. 2007), from which N_2O_5 may be derived using the equilibrium relationship [Equation (1)]. More recently, long-path DOAS instruments have been used for vertical profiling in the lowest 300 m of the atmosphere, a height interval that is difficult to access otherwise (Section 4.2). Modern long-path DOAS instruments that measure tropospheric NO₂ and NO₃ are composed of a light source, such as a xenon arc lamp (Stutz et al. 2004), and a coaxial sending/receiving telescope that transmits a collimated beam of light to an array of quartz corner-cube reflectors positioned 2-6 km away from the instrument. The reflectors send the light back to the telescope where the narrow-band absorptions of various trace gases along the light path are analyzed with a spectrograph-detector system. For NO₃, the window of wavelength is between 610 and 680 nm. To study the vertical distribution of trace gases in the lowest 100-300 m, three-five retroreflector arrays may be mounted at different altitudes. This setup allows the retrieval of concentration profiles with 2–40 m vertical resolution that are averaged across 2-6 km in the horizontal direction. This technique has been applied successfully in Houston and Phoenix (Stutz et al. 2004; Wang et al. 2006). Detection limits for NO₂ and NO₃ near the ground are typically 160 and 2 ppt, respectively, on a 5-km long light path (Platt and Stutz 2008). Applying Equation (1) at 1 ppbv of NO₂, these values translate to N₂O₅ detection limits of 900 ppt at 255 K and 0.4 ppt at 310 K. The temporal resolution is between 10 and 20 min for each complete set of measurements.

3.2. Cavity Ring-Down Spectroscopy (CRDS)

A major breakthrough in the ambient measurement of N₂O₅ occurred over the past decade with advancements in CRDS. First reported by O'Keefe and Deacon (1988), the potential of CRDS for atmospheric trace gas measurements was recognized initially by successful measurements of ambient NO2 in laboratory air (O'Keefe and Lee 1989). For further details on the technique, the reader is referred to numerous review articles (Busch and Busch 1999; Atkinson 2003; Brown 2003). King et al. (2000) demonstrated the first laboratory measurements of NO₃ by CRDS, and Brown et al. (2001, 2002) demonstrated the first in situ measurements of both NO₃ and N₂O₅ in ambient air by using CRDS. The latter system employs two mirrors of high finesse (mirror reflectivity, $R \ge 99.999\%$ at the strong, 662-nm NO₃ absorption band) and a tunable, pulsed dye laser system that injects the laser beam into the cavity directly through one of the end mirrors. This is referred to herein as pulsed CRDS. The concentration of the species of interest is determined by the decay of the laser intensity within the cavity, since the inten-

sity decay is directly proportional to the absorber concentration. Zero determination is obtained by periodic addition of NO to the inlet to destroy NO₃ via Reaction (R18). The combination of 662-nm optical extinction and chemical titration with NO has been shown to be an extremely specific method for NO₃ detection (Dubé et al. 2006). Thermal conversion of N₂O₅ to NO₃ in a second, heated channel provides simultaneous measurements of the sum of NO_3 and N_2O_5 . The measurement of N_2O_5 is obtained via the difference between the two channels. High sensitivity to NO₃ by direct absorption measurements using this single-wavelength method requires the removal of aerosol particles from the air sample via filtration, introducing potential inlet artifacts through loss of NO₃ and N₂O₅ on the filter. Artifacts due to the accumulation of reactive aerosol on the filter surface can be minimized by changing filters at regular intervals with an automated device (Dubé et al. 2006). Additional wall losses can be quantified and calibrated through standard additions and conversion of NO₃ or N₂O₅ to NO₂, which is measured in a separate CRDS channel in the same instrument (Fuchs et al. 2008). Sensitivity and accuracy of the CRDS system has improved over the past decade. Currently, the system sensitivity is as good as 0.5 pptv for NO3 and 1 pptv for N2O5 at a 1-Hz sampling frequency, with accuracy better than 12% (Dubé et al. 2006). Figure 4 shows a diagram of the instrument.

Pulsed CRDS has been deployed during several field campaigns on ships, aircraft, tall towers, and at ground sites. The instrument was first employed in March-April 2001 at a ground site in Boulder, Colorado (Brown et al. 2003b). The New England Air Quality Study (NEAQS) used the same setup in a ship-based application to measure N₂O₅ mixing ratios in a polluted marine environment off the United States east coast during the summer of 2002. In the 2004 International Consortium for Atmospheric Research on Transport and Transformation (ICARTT) study, spatial distributions and vertical profiles of N₂O₅ were obtained by installing a pulsed-CRDS system aboard an aircraft (Brown et al. 2006b, 2007a). In October 2004, Brown et al. (2007b) deployed the pulsed-CRDS system on a movable carriage on a 300-m tower in Boulder and reported vertical distributions of NO_3 and N_2O_5 with <1 m resolution. Nakayama et al. (2008) recently employed pulsed CRDS to obtain nighttime measurements of N₂O₅ in Toyokawa, Japan. The detection limit of that system was estimated to be 1.5 pptv for NO_3 and 2.2 pptv for N_2O_5 in a 100-s averaging time.

Simpson and coworkers (Simpson 2003; Ayers et al. 2005; Apodaca et al. 2008) have undertaken a parallel development of CRDS, using continuous wave (cw) diode lasers rather than a pulsed laser source. These cw CRDS systems have the advantage of much smaller size, weight, and power consumption, making them extremely versatile for use in field campaigns, as illustrated in Figure 5. However, the single CRDS channel restricts these systems to measuring only NO_3 or $NO_3 + N_2O_5$ depending on whether the thermal converter is bypassed or used. Thus, quantification of ambient N_2O_5 with this instrument requires a collocated measurement of NO_3 for a difference calculation or

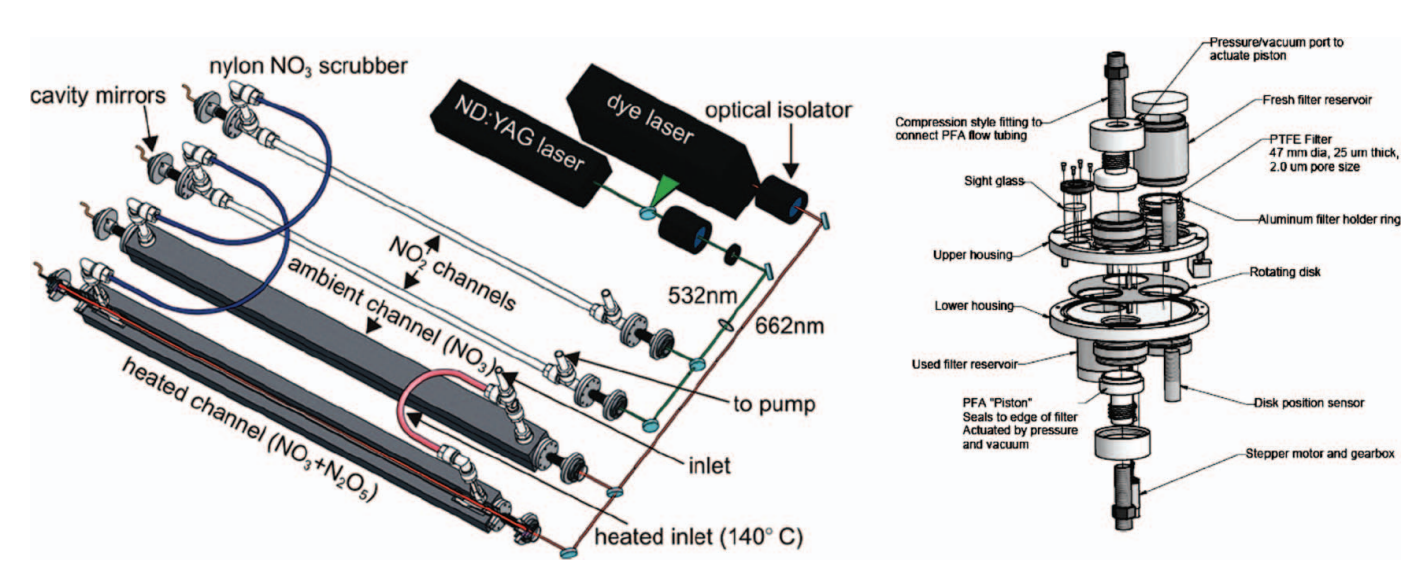


FIG. 4. Schematic of pulsed laser CRDS instrument for simultaneous measurement of NO_3 and N_2O_5 , with calibration based on conversion of these compounds to NO_2 , also measured by CRDS (Fuchs et al. 2008). Shown at right is the automated filter changer to prevent the accumulation of reactive aerosol (Dubé et al. 2006). Copyright 2008, American Chemical Society, and 2006, American Institute of Physics. (Figure provided in color online.)

 NO_2 and temperature for an equilibrium calculation. The first field-deployed cw CRDS near Fairbanks, Alaska, had a 2σ detection limit of 1.6 pptv for NO_3 or the sum of NO_3 and N_2O_5 in a 25-s averaging time (Simpson 2003). Ayers et al. (2005) reduced the detection limit to 1.4 pptv in 4.6 s by implementing an off-axis alignment that couples the cw diode laser light with a two-mirror system. Schuster et al. (2009) have also recently demonstrated detection of NO_3 and/or the sum of $NO_3 + N_2O_5$ in a single-channel system with a cw diode laser in an off-axis

configuration. This instrument achieves a sensitivity of 2 pptv in 5 s, with performance demonstrated during measurements at an environmental simulation chamber. Crowley and coworkers (2010) modified the system of Schuster et al. (2009) by introducing a second measurement cavity that allows for simultaneous measurement of NO_3 and N_2O_5 , similar to the dual-channel instruments described above. This instrument was deployed in southwestern Germany with an N_2O_5 detection limit of 4–5 ppt in a 3-s averaging time (Crowley et al. 2010).

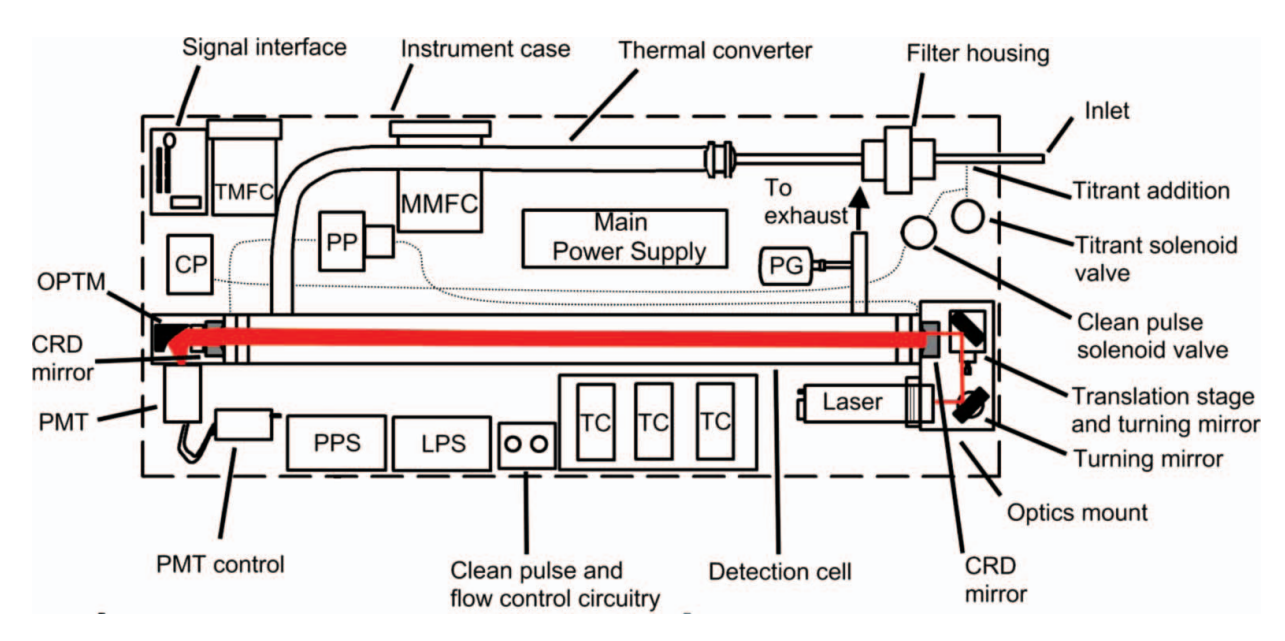


FIG. 5. Schematic of cw-CRDS instrument of Simpson (2003) for in situ detection of N_2O_5 . The instrument is designed for portability and includes a single CRDS channel with a thermal converter for measurement of the sum of NO_3 and N_2O_5 . TMFC: titrant mass flow controller; MMFC: main mass flow controller; PP: purge pump; CP: clean pulse pump; PG: pressure gauge; TC: temperature controller; LPS: laser power supply; PMT: photomultiplier tube; PPS: PMT power supply; OPTM: off-axis paraboloid turning mirror. Figure courtesy of William R. Simpson and Randy Apodaca. (Figure provided in color online.)

3.3. Broadband Cavity Ring-Down and Cavity-Enhanced Absorption Spectroscopy (CEAS)

Concurrent with the development of single-wavelength CRDS instruments that measured NO₃ by optical extinction at the center of its strong 662-nm bands was the development of broadband optical absorption methods using high-finesse optical cavities that allow spectroscopic identification of NO₃ across a much wider wavelength range (Ball and Jones 2003). Because such instruments record a complete optical spectrum over the range where NO₃ absorbs strongly, they can be used to detect NO₃ without the need for zero determination via NO addition. Furthermore, they have commonly been operated without aerosol filtering, such that analytical uncertainties due to inlet losses are significantly reduced and those due to filter aging are eliminated. The initial demonstration of these instruments employed a pulsed dye laser system operating in a broadband mode (several tens of nm bandwidth), a grating spectrometer to disperse light at the output of an optical cavity, and a clocked charge-coupled device camera to record cavity ring-down transients within multiple wavelength bins (Ball et al. 2001; Bitter et al. 2005). This instrument demonstrated sensitivity to NO₃

of 1 pptv in a 100-s integration time on a single channel and was used for ambient measurements in comparison to long-path DOAS during the 2002 NAMBLEX campaign in Great Britain (Sommariva et al. 2007).

More recent developments of this instrumentation have employed light-emitting diodes (LEDs) in place of pulsed laser systems (Ball et al. 2004; Langridge et al. 2006, 2008) in a configuration known as CEAS, in which intensity, rather than a cavity time constant, is measured (Fiedler et al. 2003). These instruments require some additional calibrations of cavity mirror losses and are thus not absolute in the same sense as CRDS. Current versions of this instrument have achieved sensitivity to NO₃ or the sum of NO₃ and N₂O₅ in a single channel of 0.25 pptv (1σ) in a 10-s average, quite comparable to the single-wavelength CRDS instruments. The extreme simplicity and low cost of the LED makes these instruments attractive for field measurements. A schematic of the Langridge et al. (2008) instrument is shown in Figure 6. These instruments have been deployed in recent ground-based field intensives in Europe, such as the RHaMBLe (Reactive Halogens in the Marine Boundary Layer) in Roscoff, France, during 2006. The single-channel broadband instruments

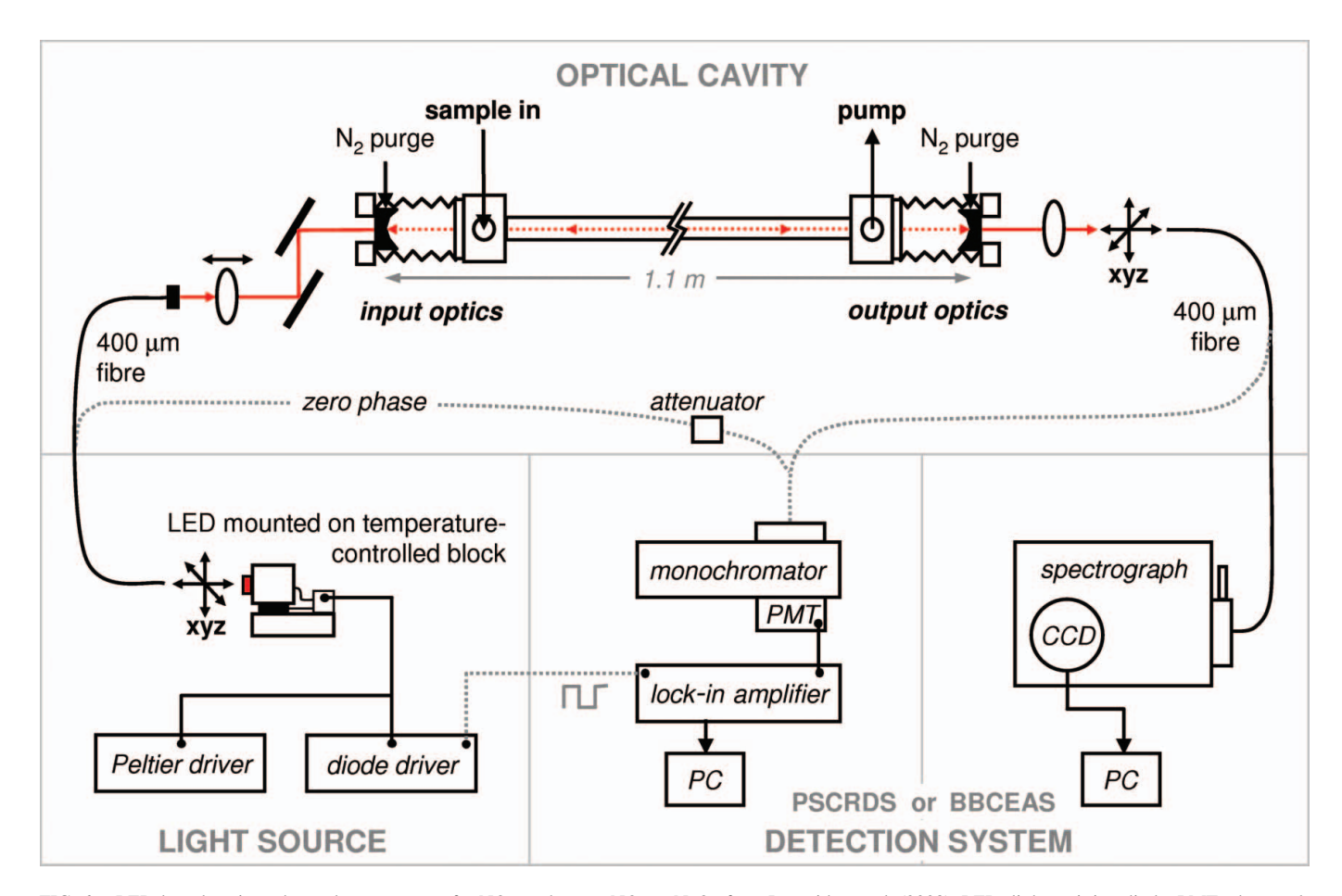


FIG. 6. LED-based cavity enhanced spectrometer for NO_3 or the sum $NO_3 + N_2O_5$ from Langridge et al. (2008). LED: light emitting diode; PMT: photomultiplier tube; PC: personal computer; CCD: charge-coupled device; PSCRDS: phase-shift cavity ring-down spectroscopy; BBCEAS: broadband cavity enhanced spectroscopy. Copyright 2008, American Institute of Physics. (Figure provided in color online.)

described here have been designed to measure the sum of NO_3 and N_2O_5 and thus would currently require a collocated measurement of NO_2 and ambient temperature to determine NO_3 or N_2O_5 individually. However, dual-channel versions of these instruments that simultaneously measure NO_3 and the sum of NO_3 and N_2O_5 are straightforward and will likely be developed in the near future.

There are a number of additional CEAS instruments whose performance has been demonstrated in environmental simulation chambers and that are likely to be used in field measurements in the near future. These include arc-lamp-based instrumentation of Venables et al. (2006) and Varma et al. (2009), which have sensitivities to NO₃ of 2–4 pptv on 5–20 m open paths within an enclosed chamber with sampling times of 5 s to 1 min. Similarly, Meinen et al. (2010) reports NO₃ detection with an LED-based CEAS instrument using DOAS retrieval techniques (Platt et al. 2009), also referred to as CE-DOAS (Table 1), to achieve a sensitivity of 6.3 pptv to NO₃ on a 1-m base path. Because these instruments have been operated in openpath configurations, they are limited to measurements of NO₃ only and require collocated measurements of NO₂ and ambient temperature in order to determine N₂O₅.

3.4. Laser-Induced Fluorescence (LIF)

LIF has been used for its accuracy and sensitivity in measuring a variety of atmospheric species, such as NO₂ and related nitrogen compounds (Thornton et al. 2000) and the HO_x radical family (Holland et al. 1995, Heard and Pilling 2003). The technique uses a laser to excite the species of interest to a higher electronic state, from which it may fluoresce with an efficiency determined by the photophysical properties of the molecule of interest. In general, the technique is extremely sensitive since photons emitted perpendicular to the excitation axis defined by the laser source can be collected and measured with high efficiency. It can also be a highly selective method since the fluorescent photons must satisfy two resonant conditions—the excitation from the laser itself and any optical filtering used to define the wavelength window over which the fluorescence is collected. The utility of LIF for particular trace gas measurements then depends on the accessibility and intensity of electronic transitions in regions where laser sources are available and the fluorescence yield.

The nitrate radical, with its strong and highly accessible visible absorption bands, would seem an ideal candidate for LIF detection of either this compound or N_2O_5 via thermal conversion, as described above. Wood et al. (2003) pioneered the use of this technique, demonstrating detection of NO_3 (or N_2O_5) in a prototype instrument that used a simple, inexpensive cw laser source (36-mW total power) that could be coarsely tuned around the strong 662-nm NO_3 absorption band. The system employed a multipass Herriot cell (approximately 40 passes), photon counting, and detection within a 700–750 nm spectral window to achieve optimal sensitivity and specificity to NO_3 . The most important contributions to the background signal (i.e.,

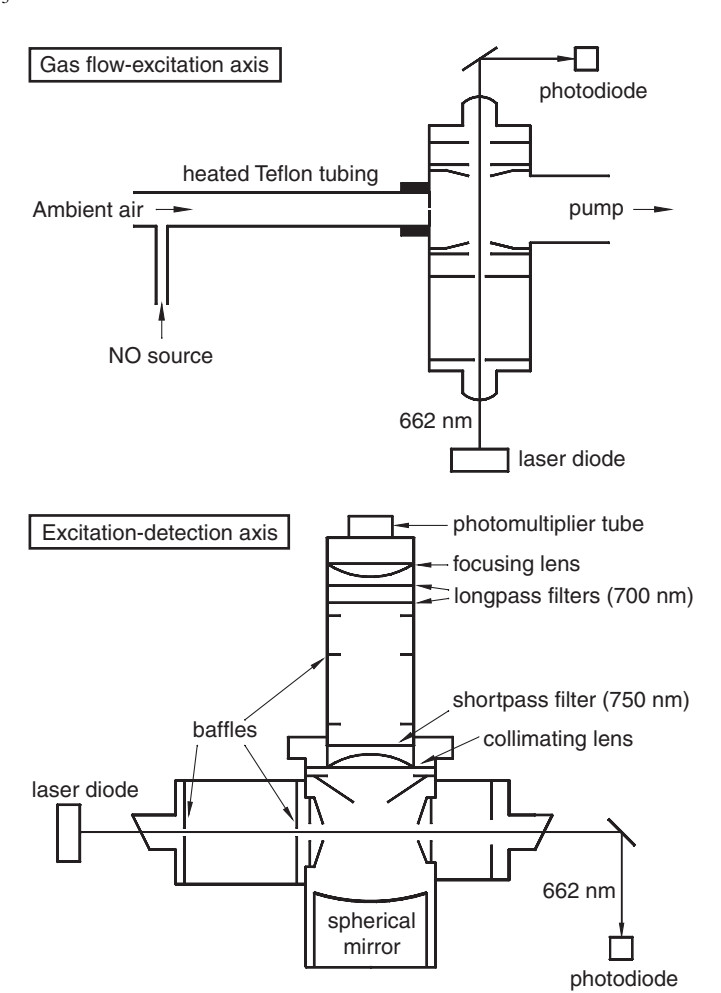


FIG. 7. LIF instrument for N₂O₅ measurement. Figure courtesy of Ezra Wood.

interferences) were due to scattering processes, such as Mie and Rayleigh scattering, scatter from the excitation laser itself, and fluorescence from NO_2 . The instrument sensitivity to NO_3 fluorescence was calibrated by conversion of NO_3 to NO_2 by reaction with NO [i.e., Reaction (R18)], followed by LIF measurement of NO_2 using a separate laser (with independent calibration of the NO_2 response). Figure 7 shows a schematic view of this instrument. A key finding was that the overall LIF sensitivity to NO_3 was some 1,600 times smaller than estimated based on comparison to similar instruments in use for NO_2 . These results implied that although the instrument was capable of selective detection of NO_3 or N_2O_5 , it likely had sensitivity sufficient for detection only of the latter, with a detection limit of 76 pptv (2σ) in a 60-s average.

Field measurements of N_2O_5 were demonstrated with this instrument during a wintertime campaign at a site on the East side of the San Francisco Bay area (Wood et al. 2005). The instrument was operated under conditions where the sum of NO_3 and N_2O_5 would be dominated by N_2O_5 , such that no NO_3 measurements were reported, and the sum was taken to be representative of N_2O_5 alone. To achieve higher sensitivity,

data were averaged to 1 h, with a detection limit of 6 pptv (2σ) in this time window. The study demonstrated lifetimes of N_2O_5 that were very short, in the range 5–30 min, implying very rapid wintertime conversion of NO_x to soluble nitrate via N_2O_5 hydrolysis.

Matsumoto et al. (2005a) developed an instrument for N₂O₅ detection, also based on thermal conversion (TC)/LIF. Their instrument operated somewhat differently and achieved somewhat improved detection sensitivity, albeit at a cost of greater experimental complexity. The key difference was the use of a higher powered (400 mW), pulsed laser system (10-kHz repetition rate) that enabled time-gated detection of the fluorescent signal to discriminate against scattered light from the excitation laser. The laser system was a pulsed Nd:YVO4/dye laser, which was large enough that the laser head itself was housed inside a laboratory, with a fiber-optic connection to the optical head where actual detection was carried out. They employed a dual-wavelength excitation scheme, with a signal wavelength resonant with the NO₃ band at 622.96 nm, and an off-resonant measurement at 618.81 nm. This scheme removed any potential interference from NO₂ fluorescence (as well as light scattering from aerosol), since the two wavelengths were chosen to have the same NO₂ absorption cross section to within 1%. As with the cw instrument of Wood et al., the instrument was calibrated against NO₂ fluorescence subsequent to the conversion of NO₃ found in the added excess NO. This instrument used the same reaction for recording an instrument zero, similar to the CRDS instruments described above. The detection limit of N2O5 in the system by Matsumoto et al. (2005b) is 6 pptv (1 σ) over an integration time of 10 min. This would correspond to roughly 38 pptv (2σ) in 1 min, or approximately a factor of two better than the cw instrument of Wood et al. The pulsed-laser instrument has been used at field campaigns to measure NO₃ + N₂O₅ in the urban atmosphere near Tokyo, Japan (Matsumoto et al. 2005a) and on an island downwind of Tokyo (Matsumoto et al. 2006).

3.5. Chemical Ionization Mass Spectrometry (CIMS)

CIMS is a versatile and well-developed measurement technique used for a variety of trace gases (Huey et al. 1995). It is based on a soft and selective ionization process resulting from a reaction between a reagent ion and the compound of interest. After the molecule—ion reaction, ions expand through an orifice into a vacuum chamber for analysis by a mass spectrometer. The choice of reagent ion can lead to specificity for detecting particular compounds, while the soft ionization tends to produce simple mass spectra with relatively little fragmentation. Fehsenfeld et al. (1975) and Davidson et al. (1978) demonstrated that the gas-phase ion-molecule reaction between N₂O₅ and halide anions yields NO₃⁻, which can be readily detected. Hanson and Ravishankara (1991) and later Abbatt and coworkers (Hu and Abbatt 1997; Thornton et al. 2003) applied this technique to study the heterogeneous uptake kinetics of N₂O₅ and ClONO₂ in the laboratory by using I⁻ as a reagent ion because it ionizes N_2O_5 with at most only a weak interference from HNO_3 .

$$I^- + N_2O_5 \rightarrow NO_3^- + INO_2.$$
 [R21]

The I⁻ reagent also ionizes NO₃ to NO₃⁻, so the technique cannot differentiate between NO₃ and N₂O₅. Iodide-based CIMS methods were first applied in field studies by Huey and coworkers (Slusher et al. 2004). Figure 8 illustrates the basic schematic of the apparatus. I- is generated from a small flow of CH₃I passed over a ²¹⁰Po source. The ion-molecule reactions take place in a flow tube maintained at 20 Torr, followed by a collisional dissociation chamber (CDC), which consists of an electric field that accelerates the product ions through a gas at <0.5 Torr to break up clusters and simplify the mass spectrum. Because the principal application of this instrument is the speciation of peroxy acteyl nitrate (PAN) compounds, which requires thermal dissociation (TD) of PAN prior to the ion-molecule reaction, the instrument uses a heated inlet (TD-CIMS). Calibration of the instrument for N_2O_5 is estimated from the known sensitivity to PAN. Although the TD step is not technically required to measure the sum of $NO_3 + N_2O_5$ (because I⁻ reacts with either species to produce NO₃⁻), it is convenient since the addition of NO to the inlet provides a zero in the same fashion as the optically based N₂O₅ instruments described above. A principal drawback of this TD-CIMS method is that although I⁻ is a reasonably specific reagent ion for either NO₃ or N₂O₅, there is significant and potentially variable background noise at the 62 mass (NO₃⁻ amu). In some regions of the atmosphere, there may be additional interference from the reaction of I⁻ with ClONO₂ or BrONO₂, which also yields NO_3^- . The estimated TD-CIMS detection limit for $NO_3 + N_2O_5$ is 12 pptv in 1 s. The instrument was deployed for field measurements in Boulder, Colorado, during October 2002 (Slusher et al. 2004), which revealed high variability in N₂O₅ with an increasing trend throughout the night and rapid depletion after sunrise. A field comparison between the TD-CIMS and pulsed CRDS (Dubé et al. 2006), in which both instruments were calibrated independently, exhibited high correlation between the instruments (under conditions where the sum of $NO_3 + N_2O_5$ was dominated by N₂O₅), though the TD-CIMS consistently reported 30% less N₂O₅ than CRDS (see Figures 9a and 9b).

Ion-drift CIMS (or ID-CIMS) is a similar apparatus that has also been applied to detect N_2O_5 in the atmosphere by using I^- as a reagent ion. The basis of this technique is the use of an ion drift tube in which the time for ion-molecule reactions to occur is well constrained, such that the signal can be calibrated based on a known ion-molecule reaction rate coefficient (Fortner et al. 2004). Zheng et al. (2008) demonstrated this method for N_2O_5 (and HNO_3 , via separate reagent ion chemistry) detection during field measurements in Mexico City in 2006. The instrument was similar in many respects to that of Slusher et al. (2004), except that it did not employ a heated inlet and so it measured N_2O_5 directly via Reaction (R9). The instrument was

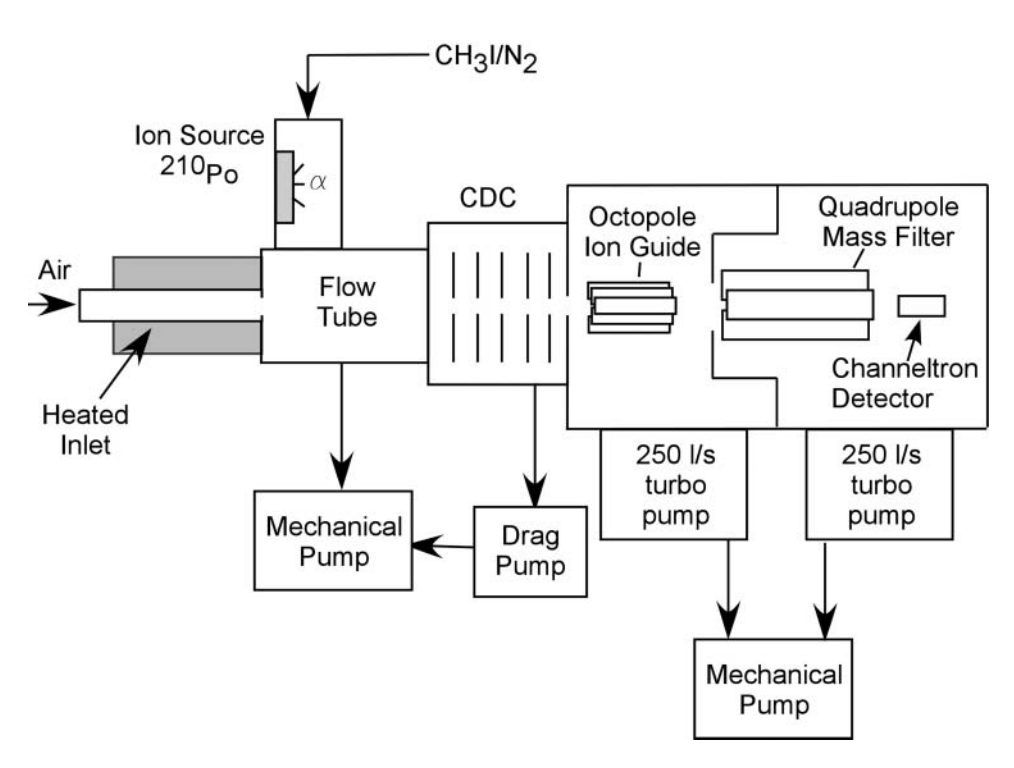


FIG. 8. Chemical ionization mass spectrometer for N₂O₅ detection. CDC: collisional dissociation chamber (Adapted from Slusher et al. 2004).

zeroed by shunting the ambient air flow through a heated tube to dissociate N_2O_5 into NO_3 , followed by addition of NO to the inlet. Calibrations were performed separately in the laboratory from prepared samples of N_2O_5 that were characterized by a commercial ultraviolet spectrometer. The reported detection limit is 30 pptv (3σ) for a 10-s averaging time (Zheng et al. 2008).

The University of Washington CIMS (UW-CIMS) is similar to the TD-CIMS, but it has an ion-molecule reaction region (IMR) in place of the heated inlet and flow tube. By removing the heated inlet, N_2O_5 molecules remain intact and can be directly measured rather than the sum of $NO_3 + N_2O_5$. In the IMR, neutral molecules are allowed to react with I^- ions for \sim 70 ms (Kercher et al. 2009). The novelty of this technique is its lack of high and variable chemical interferences because it detects iodide-containing clusters,

$$I^- + N_2O_5 \rightarrow I(N_2O_5)^-,$$
 [R22]

rather than nitrate anions. The $I(N_2O_5)^-$ cluster is an intermediate in the ion–molecule reaction leading to nitrate formation and must be detected before it dissociates so that the instrument can distinguish N_2O_5 from other sources of NO_3^- [compare Reactions (R21) and (R22)]. Formation of this cluster is optimized in the UW-CIMS by tuning the flow-tube pressures and the CDC voltage. This instrument was deployed on a research vessel at the International Chemistry in the Arctic Lower Troposphere (ICEALOT) campaign and demonstrated a detection limit of \sim 5 pptv. Prior to the ICEALOT campaign,

the UW-CIMS performance was tested against pulsed CRDS in Boulder, Colorado. Results of that intercomparison, plotted in Figures 9c and d, show excellent agreement between the two measurement techniques. However, unlike the intercomparison plotted in Figures 9a and b, the UW-CIMS calibration was based partly on a direct comparison with the CRDS calibration source (Fuchs et al. 2008).

4. FIELD OBSERVATIONS OF N₂O₅

Determinations of ambient N_2O_5 levels have been available for at least 25 years by equilibrium calculations from simultaneous measurements of NO_3 and NO_2 by long-path DOAS (Atkinson et al. 1986), and direct in situ observations have been available since 2001 (Brown et al. 2001). Since a comprehensive review of all field measurements is beyond the scope of this article, we summarize several key findings in this section from recent field studies using in situ methods or vertically resolved DOAS. These include recent advances in our knowledge of N_2O_5 chemistry in cold climates, its vertical distribution in the lower atmosphere, and the rate of and reaction products from N_2O_5 heterogeneous hydrolysis.

4.1. N_2O_5 Levels in the Atmosphere

Since the discovery of the NO_3 radical in the atmosphere of Southern California in 1979, studies have speculated about the levels of N_2O_5 and its potential impact on the nocturnal NO_x budget. Calculated equilibrium N_2O_5 mixing ratios in these initial studies were reported at 1.5–14 ppb in polluted air (Platt et al. 1980; Atkinson et al. 1986), while long-term measurements

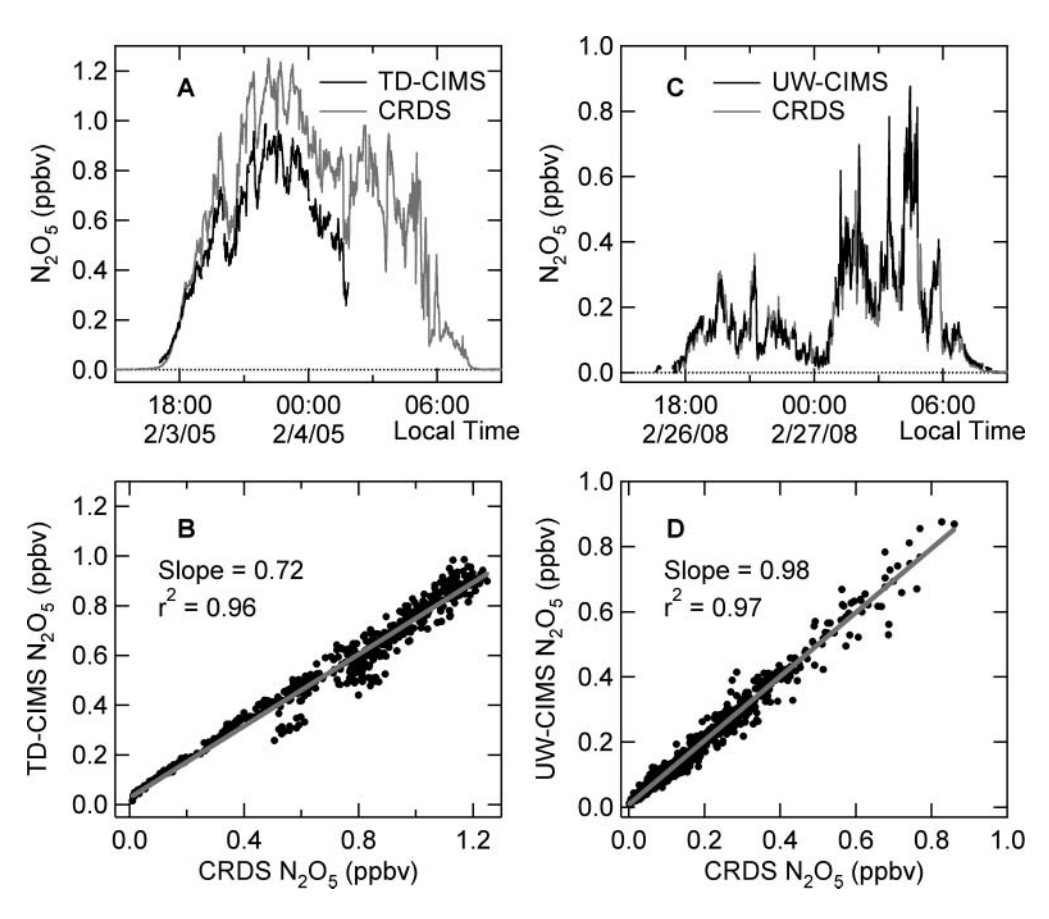


FIG. 9. Data from two separate intercomparisons between CIMS and CRDS instruments sampling ambient air in Boulder, Colorado. (a, b) A February 2005 comparison between the TD-CIMS instrument (Slusher et al. 2004), based on NO_3^- , with the pulsed CRDS instrument (Dubé et al. 2006). The TD-CIMS data have an arbitrary offset that has been subtracted. (c, d) A February 2008 comparison of the UW-CIMS, based on $I \bullet N_2 O_5^-$, with the same pulsed CRDS instrument. Data in both comparisons are plotted at approximately 1-min time resolution. TD-CIMS data courtesy of Greg Huey, Frank Flocke, and Aaron Swanson. UW-CIMS data courtesy of James Kercher and Joel Thornton.

in marine and continental areas in Europe found up to 3.8 ppb of N₂O₅ (Heintz et al. 1996; Geyer et al. 2001). Analyses of longterm data show distinct seasonal variations in the N2O5 loss pathways, with direct loss of N₂O₅ most important in winter and indirect loss via NO₃ of greatest importance in summer (Heintz et al. 1996; Allan et al. 1999; Geyer et al. 2001; Vrekoussis et al. 2007). Other shorter field observations, including the in situ measurements by Brown et al. (2003b, 2006b, 2007b), have generally confirmed the presence of a few ppb of N₂O₅ in the troposphere. Atmospheric observations have confirmed that the equilibrium Reaction (R2) holds for most conditions during summertime (Perner et al. 1985; Brown et al. 2003b; Osthoff et al. 2007; Crowley et al. 2010), suggesting that the larger body of data that inferred N₂O₅ from NO₂ and NO₃ is likely valid in warm conditions. Field data have also given important insights into atmospheric N₂O₅ chemistry, including the role of N₂O₅ uptake as an NO_x loss mechanism (Geyer et al. 2001; Stutz et al. 2004) and the N₂O₅ lifetime during summer (see Section 4.3).

In cold environments (e.g., high latitudes, high altitudes, and/or winter months), it becomes difficult to infer N_2O_5 mixing

ratios from NO₃ because the equilibrium reaction (R2) shifts strongly in favor of N₂O₅ (Figure 1) and the NO₃ levels often drop below detection limits. Under such conditions, in situ measurement techniques are critical to determining the N₂O₅ mixing ratio. At a polluted Arctic site during winter, Apodaca et al. (2008) observed N₂O₅ levels as high as 50–100 ppt. This study and a previous study at similar conditions by Ayers and Simpson (2006) estimated N₂O₅ lifetimes from below 1 min up to 4 h. These short lifetimes are indicative of a fast, direct loss of N₂O₅ because NO₃ levels are so low at cold temperatures. Apodaca et al. (2008) argue that N₂O₅ is predominately lost on snow or ice particles. The dark reaction of NO₂ with O_3 to produce N_2O_5 is a more important mechanism for NO_x loss in wintertime, when daytime NO_x loss, driven by the reaction of NO₂ with photochemically produced OH radicals, is significantly reduced.

4.2. N₂O₅ Vertical Distribution

Weak vertical mixing in the nighttime boundary layer (NBL), which often is shallower than $\sim\!200$ m, leads to an accumulation of freshly emitted pollutants (e.g., NO) near the surface.

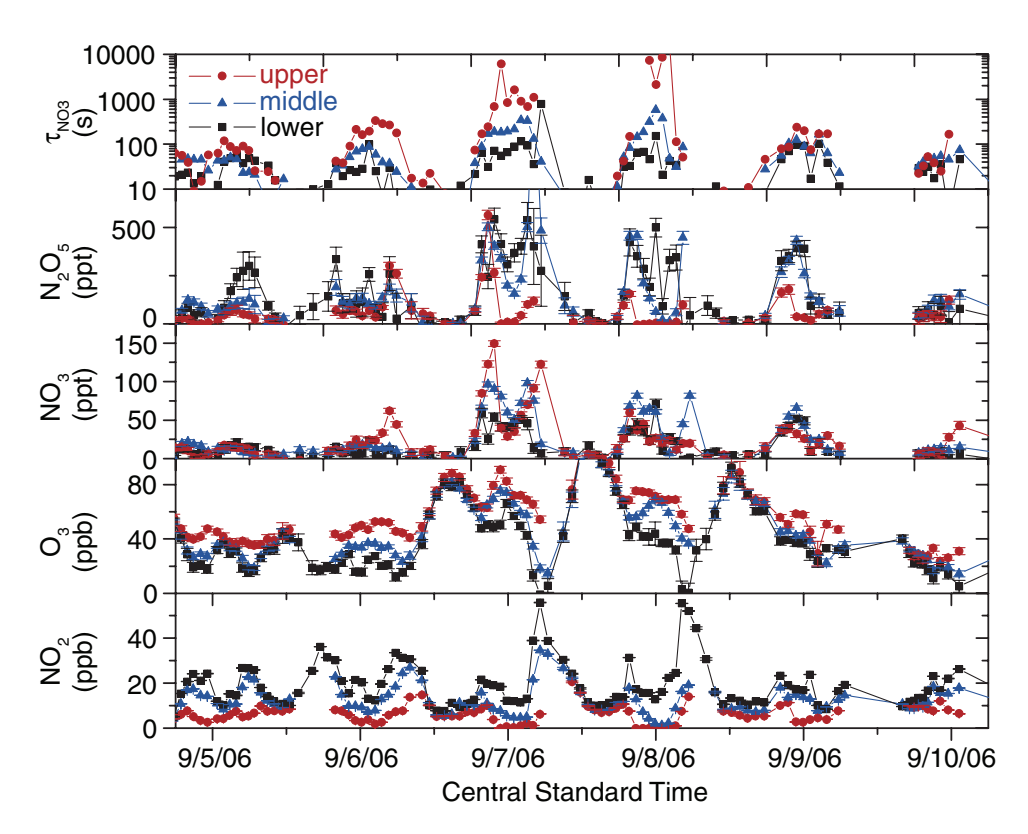


FIG. 10. Vertical profiles of various atmospheric trace gases in Houston, Texas, measured by long-path DOAS in September 2006. Data are shown in three height intervals: lower (20–70 m), middle (70–130 m), and upper (130–300 m). (Adapted from Stutz et al. 2009.) (Figure provided in color online.)

This can result in efficient titration of NO₃ by NO [Reaction (R18)], as well as titration of O₃ by NO, leading to complex vertical concentration gradients in NO₃, N₂O₅, and their source gases, as well as a very altitude-dependent chemistry. By using DOAS measurements of scattered solar light during sunrise, von Friedeburg et al. (2002) were able to construct one of the first vertical profiles of tropospheric NO₃. It exhibited a maximum at \sim 300 m, the height where nocturnal jets are capable of carrying N_2O_5 overnight to downwind distance of ~ 300 km. Since their technique did not allow the simultaneous measurement of NO₂ profiles, equilibrium N₂O₅ concentration profiles could not be derived. Stutz et al. (2004) used long-path DOAS on several vertically arranged light paths to simultaneously measure NO₃ and NO₂ and calculated equilibrium N₂O₅ profiles in the lowest 120 m of a suburban atmosphere near Houston during the Texas Air Quality Study (TexAQS) in 2000. For several nights, NO₃ and N₂O₅ exhibited negligible levels at the surface but reached 100 and 300 ppt, respectively, between 100 and 120 m altitude. Other studies in the urban NBL reveal similar vertical profiles (e.g., Wang et al. 2006).

Figure 10 presents sample concentration profiles of NO_2 and NO_3 in three height intervals over a 1-week period during the second TexAQS in 2006 (Stutz et al. 2009). The measurements were taken in coastal regions where strong internal boundary layers form, characteristic of areas near large bodies of water.

During all nights, NO2 exhibits higher levels near the surface and lower mixing ratios aloft, while ozone shows the opposite behavior. In general, NO₃ levels in the lower NBL (20–130 m altitude) show the expected profile of low NO₃ near the surface due to Reaction (R18), while N₂O₅ tends to be lowest above the NBL due to the very low NO₂ mixing ratios in the residual layer (see gray circles in the N₂O₅ panel of Figure 10). Peak levels of calculated steady-state N₂O₅ were observed mostly in the lower or middle height interval, reaching up to 500 pptv. Such drastic variations in N₂O₅ levels show a clear vertical gradient during many nights of the measurement campaign. The vertical profile of N₂O₅ is further complicated due to its dependence on aerosol concentration profiles [Equation (4)], RH [via Reaction (R3)], and the vertical temperature gradient [Equation (1)]. Vertical profiles of N_2O_5 within and above the NBL were also observed by in situ measurements at a tall tower in Boulder, Colorado (Brown et al. 2007b), and also showed strong vertical gradients. In this study, such gradients were particularly sharp within the surface layer (approximately the lowest 20 m), again most likely due to Reaction (R18). These observations showed large variability, with N₂O₅ maxima up to 2 ppbv and distinct layering of N₂O₅ at certain times during the night.

The recent development of sensitive in situ techniques to measure NO_3 and N_2O_5 allowed further investigation of N_2O_5 chemistry in the residual layer and free troposphere. Aircraft

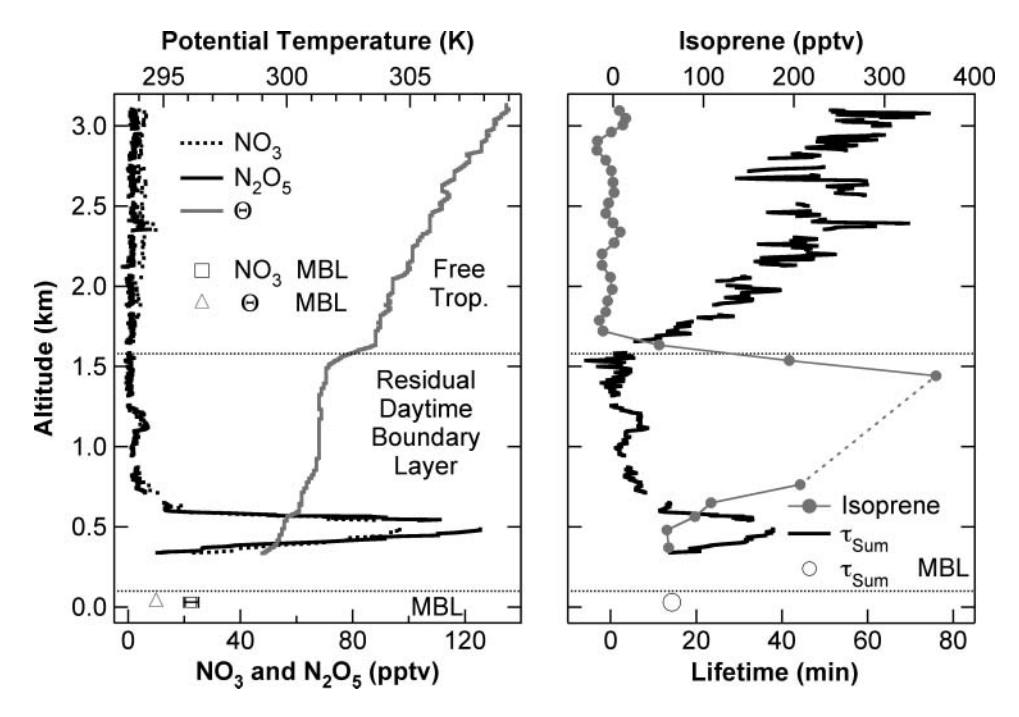


FIG. 11. Aircraft vertical profiles of NO_3 , N_2O_5 (measured by CRDS), potential temperature (Θ), isoprene, and $NO_3 + N_2O_5$ lifetime (τ_{Sum}), and surface-level measurements of NO_3 (measured by DOAS), Θ , and τ_{Sum} off the New Hampshire coastline in August 2004 (adapted from Brown et al. 2007a). Different symbols are used to distinguish measurements made in the marine boundary layer (MBL) from those collected in the aircraft, as indicated in the legends.

data, sometimes in combination with surface observations, often show an increase of NO₃ and N₂O₅ with altitude in the lowest 500 m of the nocturnal atmosphere, but the direction of the gradient may be reversed due to variations in pollutant compositions and the stability of the atmosphere. Figure 11 shows one example profile taken near the New Hampshire coastline in August 2004. A DOAS instrument with a light path between two islands provided surface-level measurements of NO₃ (and calculated N₂O₅, not shown). The aircraft navigated a spiral ascent to just over 3 km. The altitude dependence of the NO₃ + N_2O_5 lifetime $[(\tau_{Sum} = [NO_3 + N_2O_5]/(k_1[NO_2][O_3]))]$, where k_1 is the reaction rate coefficient of Reaction (R1)] shows three distinct chemical regimes correlated with the layered structure in the potential temperature profile, including (1) the marine NBL, likely dominated by reactions of NO₃ with DMS emitted from the ocean (R19); (2) the residual daytime boundary layer, containing considerable level of isoprene (hence high rates of an indirect N₂O₅ loss pathway) advected offshore from the land surface; and (3) the free troposphere, where NO₃ and N₂O₅ have small production rates but long lifetimes. Even within the residual daytime boundary layer, additional stratification and concentration gradients are evident, such as the distinct plume near 500-m altitude (Brown et al. 2007a). On the basis of observed enhancements in tracers such as CO and SO₂ (not shown), this plume appears to have been of urban origin. It was likely not measured at surface level in this profile due to the interaction of the marine and terrestrial boundary layers in this region.

4.3. Field Determinations of the N₂O₅ Uptake Rate

Recent advances in the measurement of N₂O₅ from mobile platforms and direct measurements of N2O5 reactivity have provided new insight into the efficiency of its heterogeneous uptake in different parts of the troposphere and the factors governing that process. Brown et al. (2006a, b, 2009) analyzed in situ aircraft measurements of N2O5 by pulsed CRDS from the ICARTT campaign (Fehsenfeld et al. 2006) and the second TexAQS (Parrish et al. 2008) to quantitatively determine $\gamma_{N_2O_5}$. The analysis method relies on the assumption of a steady state in NO₃ and N₂O₅ with respect to their production and loss (Brown et al. 2003a). Scaling of the steady-state lifetimes [or the ratio of measured concentrations to production rates from Reaction (R1)] with NO_x within discrete plumes transected by a ship or aircraft provides a method to separate and quantify individual sinks for either NO₃ or N₂O₅ (Brown et al. 2009). The first key result from these studies is that $\gamma_{N_2O_5}$ values show considerable spatial variability (Brown et al. 2006b). For example, during a nighttime flight across the northeast US during ICARTT, lifetimes of N2O5 were found to be short in Region I, but considerably longer in Region III along the East Coast (Figure 12). All of the variability in N₂O₅ lifetimes is attributable to the rate of N₂O₅ uptake rather than to indirect loss via NO₃ chemistry. Plumes sampled in Region I exhibited $\gamma_{N_2O_5}$ values of 0.02, while those along the East Coast had $\gamma_{\rm N_2O_5} \leq 0.002$. This tenfold difference significantly affected nocturnal NO_x lifetimes in the two regions, with 93% predicted overnight NO_x loss in Ohio but only 50% in New England.

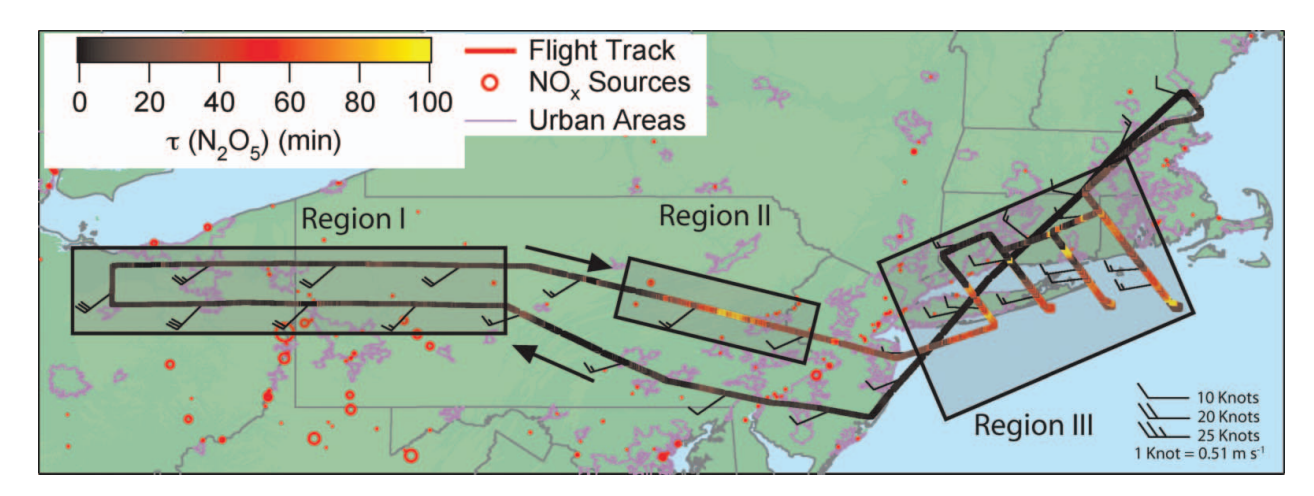


FIG. 12. Flight track of NOAA P-3 aircraft during a night in August 2004. The track is color coded by the observed lifetime of N_2O_5 , $\tau(N_2O_5) = [N_2O_5]/k_1[O_3][NO_2]$, where k_1 is the rate coefficient of Reaction (R1). The map indicates both power-plant and urban NO_x sources and the areas over which the N_2O_5 uptake coefficient was observed to vary regionally (Brown et al. 2006b). Reprinted with permission from AAAS. (Figure provided in color online.)

A second key result is that the values of $\gamma_{N_2O_5}$ seen in field studies were often smaller than those derived from laboratory measurements on pure inorganic salts, particularly along the East Coast, where neutral ammonium sulfate was the principal aerosol component. However, the field determinations are consistent with more recent laboratory measurements on mixed organic/inorganic systems discussed in Section 2.1. Determinations of $\gamma_{N_2O_5}$ from flights during the ICARTT campaign that had mixed organic/inorganic aerosol showed values generally smaller than 0.005.

The analysis of ICARTT and TexAQS aircraft measurements also indicated that the homogeneous hydrolysis rate coefficients recommended for Reaction (R3) and the corresponding third-order reaction (Section 2.1) on the basis of chamber studies appear to be too large (Brown et al. 2006b, 2009). While a recent field study in Germany supports this finding (Crowley et al. 2010), others have found that the inclusion of Reaction (R3) is necessary for models to accurately reproduce the observed NO₃ levels in a marine environment (Ambrose et al. 2007). Further field and laboratory work are needed to resolve these discrepancies.

More recent field measurements have investigated the reactivity of N_2O_5 directly using ambient flow-tube measurements in much the same manner that OH reactivity has been determined. These experiments were carried out using UW-CIMS detection of N_2O_5 (Section 3.5) coupled to a flow-tube reactor in which an artificial source of N_2O_5 is injected at the entrance, and the amount of N_2O_5 exiting the flow tube is measured in air samples that are alternately filtered and unfiltered of ambient particles (Bertram et al. 2009). Because the rate coefficient for N_2O_5 loss is relatively slow, the residence time in the flow tube must be much longer than needed for OH reactivity determinations in order to obtain a meaningful N_2O_5 loss rate coefficient. Although these measurements have so far been carried out

only at surface locations, their advantage over the steady-state method from aircraft transects is that they provide a larger number of measurements with which it is possible to statistically assess the factors that govern N_2O_5 reactivity. As an example, Figure 13 shows some values of $\gamma_{N_2O_5}$ determined via the UWCIMS method during summer months at a low-RH (15%–45%) field site, Boulder, and a high-RH (61%–87%) field site, Seattle (Bertram et al. 2009). The comparison between measurements from the two sites not only showed strong dependence of $\gamma_{N_2O_5}$ on RH, the influence of varying aerosol organic-to-sulfate ratios is also prominent.

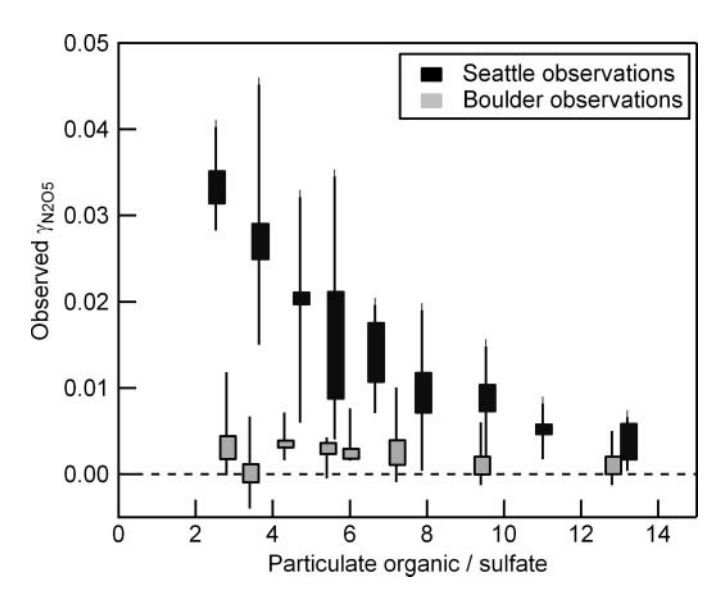


FIG. 13. Observed ambient $\gamma_{N_2O_5}$ with associated particulate organic-to-sulfate ratios at two field sites: Boulder (RH = 15%–45%) and Seattle (RH = 61%–87%). (Adapted from Bertram et al. 2009.)

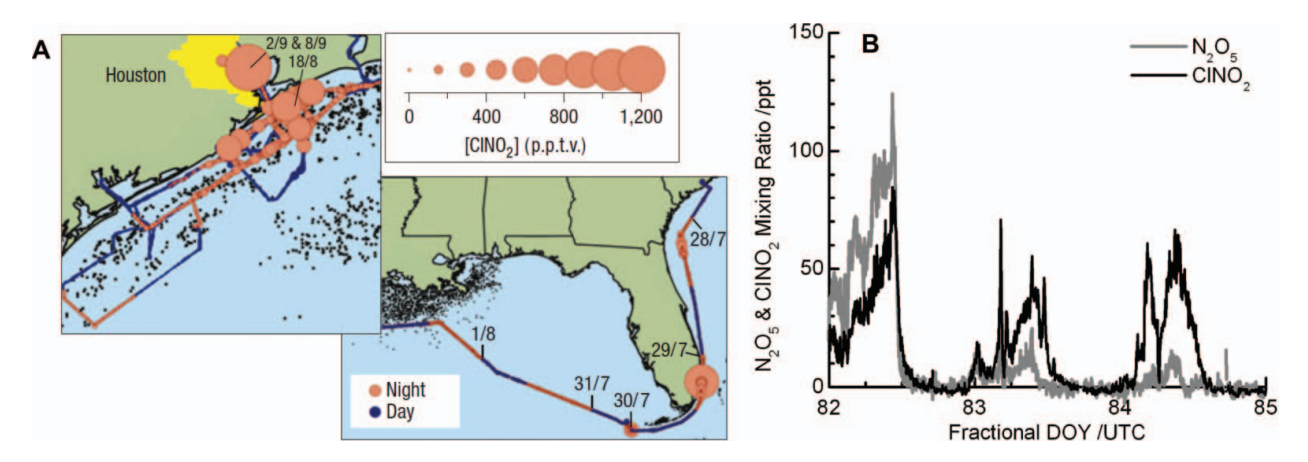


FIG. 14. (a) Map of the ship track of the R/V Brown during the second TexAQS campaign in 2006, color coded to show night and day, and size coded by the observed mixing ratio of ClNO₂ (Osthoff et al. 2008). Reprinted by permission from Macmillan Publishers Ltd.: *Nature Geosciences*, copyright 2008. (b) The ClNO₂ and N₂O₅ mixing ratios measured from 22 March 2008 (DOY 82) through 24 March 2008 during the ICEALOT field campaign (From Kercher et al. 2009). (Figure provided in color online.)

4.4. Field Determinations of $CINO_2$ Production through N_2O_5 Heterogeneous Uptake

The product branching in N₂O₅ uptake is another key issue recently elucidated by field measurements. Most current atmospheric models that consider N₂O₅ heterogeneous uptake (Evans and Jacob 2005; Foley et al. 2010) treat HNO₃ as the only product [i.e., Reaction (R4)] and do not consider nitryl halide formation via Reaction (R12). Recent direct field measurements of nitryl chloride, ClNO₂, have shown that it is produced in surprisingly large quantities from reactive uptake of N₂O₅, implying that nighttime heterogeneous chemistry may be a larger source of tropospheric halogen activation than previously recognized (Osthoff et al. 2008; Thornton et al. 2010). Previous estimates of the branching, based largely on the assumption that HNO₃ and ClNO₂ production occurred via uptake to submicron and supermicron (i.e., sea salt) aerosol, respectively, suggested that the production of ClNO₂ should be relatively modest, amounting to some tens of pptv in integrated overnight production in a polluted coastal environment (Aldener et al. 2006) or a global source of roughly 0.06 Tg Cl annually (Erickson et al. 1999). Recent ship-based measurements of N₂O₅ and, for the first time, ClNO2, during a 2006 campaign along regionally polluted areas of the US Gulf Coast, demonstrated that ClNO2 occurs routinely at hundreds of pptv and occasionally ppbv levels (Figure 14a). Production of this order could be explained by invoking a relatively large yield of ClNO₂ on both sea-salt and submicron aerosols, suggesting that a significant fraction of total N₂O₅ consumption in polluted marine and coastal environments goes to the production of this gas-phase halogen compound. A revised global source estimate suggests annual Cl production of roughly 3.2 Tg in coastal and marine environments (Osthoff et al. 2008) and up to 22 Tg if continental areas are also included (Thornton et al. 2010). Such estimates comprise a large fraction of current global budgets for tropospheric chlorine (Platt et al. 2004; Allan et al. 2007).

The 2006 results were from a late-summer campaign in a polluted subtropical marine boundary layer. More recent results from a second, ship-based campaign in late-winter 2008 (ICEALOT, http://saga.pmel.noaa.gov/Field/icealot/ index.html) along coastal areas of the Northeast US and the North Atlantic have also shown efficient ClNO₂ production from shipping channels and coastal urban sources of NO_x. Similar simultaneous measurements of both N₂O₅ and ClNO₂ in the Long Island Sound and other locations downwind of the Northeast US corridor showed significant amounts of both compounds, with ClNO₂ levels generally exceeding those of N₂O₅, as shown in Figure 14b (Kercher et al. 2009). Surprisingly, detectable levels of ambient ClNO2 are not limited to coastal environments. Thornton et al. (2010) collected measurements near Boulder, Colorado, and found as much as 100-450 pptv of ClNO₂ in urban plume samples. These peaks correlated well with high mixing ratios of N₂O₅ occurring at night and early morning. Moreover, Thornton and coworkers estimated that more than half of the predicted ClNO₂ production in the United States occurs over land. Thus, ClNO₂ formation appears to be an important product of N₂O₅ heterogeneous uptake in a variety of environments, warranting further investigation of its production mechanisms.

5. MODELING TROPOSPHERIC N₂O₅

With increasing attention on laboratory and ambient measurements of N_2O_5 and its loss pathways, the modeling community has been working in parallel to understand the driving forces behind observed vertical gradients and regional distributions of N_2O_5 to quantify its impact on NO_x budgets and nitrate formation (Galmarini et al. 1997; Riemer et al. 2003). One of the major uncertainties in modeling ambient N_2O_5 is the parameterization of $\gamma_{N_2O_5}$. Results from both laboratory experiments and ambient measurements have shown that $\gamma_{N_2O_5}$ varies by several orders of magnitude, depending on the

prevailing meteorological conditions and aerosol composition (Sections 2.1 and 4.3). Also, the importance of homogeneous hydrolysis relative to heterogeneous hydrolysis is in question (Section 4.3). These uncertainties lead to further uncertainties in our understanding of the oxidizing capacity and pollutant levels in the troposphere, especially during nighttime. In particular, the NO_x and volatile organic compound (VOC) budgets as well as aerosol loading and composition are closely linked to N_2O_5 levels at night, as outlined in Figure 2 and Section 2.

5.1. Model Representation of N₂O₅ Uptake

When only homogeneous hydrolysis is considered, Emmerson and Evans (2009) showed that the reaction between N₂O₅ and H₂O contributes to a significant portion of uncertainties and discrepancies in inorganic chemistry among various gas-phase tropospheric chemistry schemes. Dimitroulopoulou and Marsh (1997) suggested adding a temperature dependence to the rate of Reaction (R3) based on early DOAS estimates of ambient N₂O₅ (Atkinson et al. 1986). This temperature-dependent function was implemented in the Particulate Matter Comprehensive Air Quality Model with eXtensions (PMCAMx) model for a study of seasonal pollutants variation in the eastern United States to avoid overprediction of HNO₃ level (Karydis et al. 2007). An early approach for modeling heterogeneous N₂O₅ hydrolysis in the troposphere was to treat it as a first-order loss reaction that produces HNO₃ (Russell et al. 1985; Chang et al. 1987; Hov et al. 1988), without explicitly modeling the aerosol surface area needed in Equations (3) and (4). Later, modeling studies incorporated N_2O_5 uptake by particle surfaces, assuming $\gamma_{N_2O_5}$ has a constant value of 0.1 (Dentener and Crutzen 1993; Pleim et al. 1995). Dentener and Crutzen (1993) found that by including the heterogeneous uptake of N₂O₅ and NO₃, the modeled yearly average global NO_x burden decreased by 50%. Similar results of up to 60% HNO₃ increase and 50% NO_x decrease were reported in a regional modeling study of the Houston-Galveston area where heterogeneous uptake with the same constant $\gamma_{N_2O_5}$ value of 0.1 was considered only on sulfate aerosols (Lei et al. 2004). However, Dentener and Crutzen (1993) forewarned that the laboratory measurements of $\gamma_{N_2O_5}$ varied by two orders of magnitude, and their estimate of 0.1 was an upper limit. In a more recent modeling study, Bauer and coworkers (2004) parameterized an RH-dependent $\gamma_{N_2O_5}$ function on mineral dust (0.02 at RH = 70% and 0.003 for RH = 30%) and showed that such uptake alone accounts for approximately 11% of global N₂O₅ loss, contributing as a major source of HNO₃.

There are several proposed mechanistic explanations for the variability of $\gamma_{N_2O_5}$ on the basis of aerosol composition and ambient conditions (refer to Section 2.1 for detailed discussions), but the associated rate constants for these reaction pathways remain highly uncertain. Thus, one way to develop $\gamma_{N_2O_5}$ as a function of environmental variables and aerosol mix is to rely on regression models to fit laboratory data (Evans and Jacob 2005; Davis et al. 2008). In an effort to improve model predictions

of the impact of N_2O_5 heterogeneous uptake while maintaining computational efficiency, Evans and Jacob (2005) implemented laboratory-based parameterizations of $\gamma_{N_2O_5}$ for five aerosol types: sulfate, organic carbon, black carbon, sea salt, and dust. For some of these aerosol types, $\gamma_{N_2O_5}$ was specified as a function of temperature and RH. Using the GEOS-CHEM global chemical transport model, they showed a 7% increase in the tropospheric NO_x burden when the updated parameterizations of $\gamma_{N_2O_5}$ were used in lieu of a constant value of 0.1. In addition, a significant increase in both global N2O5 and NO3 concentrations was reported, resulting in an increase in ambient OH, which led to an overall increase in ozone concentration. More recently, Alexander et al. (2009) used the GEOS-CHEM model in conjunction with the N₂O₅ hydrolysis treatment presented by Evans and Jacob (2005) to model the oxygen isotopic composition (Δ^{17} O) of nitrate and to estimate different pathways of nitrate formation. Their study showed that N₂O₅ hydrolysis contributes to 18% of the global annual-mean tropospheric inorganic nitrate and 74% at high northern latitudes over the continents and the Arctic.

Relative to the global-scale model simulations described above, more detailed treatments of N_2O_5 heterogeneous hydrolysis have been attempted in urban- and regional-scale modeling studies. In order to account for the suppression of $\gamma_{N_2O_5}$ when nitrate is present in the particles, Riemer et al. (2003) introduced the following parameterization:

$$\gamma_{\text{N}\leq\text{sub}\geq2\leq\text{sub}\geq5\leq\text{sub}>,\text{mix}} = f \cdot \gamma_1 + (1-f) \cdot \gamma_2,$$
 [5]

with $\gamma_1 = 0.02$, $\gamma_2 = 0.002$, and

$$f = \frac{m_{\rm SO_4}}{m_{\rm SO_4} + m_{\rm NO_3}},\tag{6}$$

where $m_{\rm SO_4}$ and $m_{\rm NO_3}$ are the particle-phase mass concentrations of sulfate and nitrate, respectively. While Riemer et al. (2003) modeled the nitrate effect as a full order of magnitude suppression of $\gamma_{\rm N_2O_5}$, studies on ammoniated salts showed that suppression to be between a factor of 1.3 and 5.2 (Davis et al. 2008).

Davis et al. (2008) developed a parameterization for $\gamma_{N_2O_5}$ on inorganic aerosols as a function of composition of the particle-phase state of the aerosol, RH, and temperature through a comprehensive examination of several laboratory studies (Table 2). The original $\gamma_{N_2O_5}$ parameterization on aqueous sulfate particles as a function of RH proposed by Davis et al. (2008) is similar to the parameterization by Evans and Jacob (2005). Due to the unconfirmed experimental values at high RH, however, Davis and coworkers recommended an "alternative" parameterization that limits the uptake probability above the threshold RH (46%) to $\gamma_{N_2O_5}(RH=46\%)$. Davis and coworkers also recommended the introduction of temperature dependence for aqueous NH₄HSO₄ particles, where the uptake reaction probability can vary by an order of magnitude from 291 to 308 K,

TABLE 2 Summary of parameterization methods for N_2O_5 heterogeneous reaction probability ($\gamma_{N_2O_5}$) on particles of different compositions. Detailed description of the parameter constants for each method can be found in Sections 2.1 Direct Loss

Pathways and 5.1 Model Representation of N₂O₅ Uptake

Particle Type	Parameterization	Parameters	Reference
Sulfate	$\gamma_{\rm N_2O_5} = \alpha \times 10^{\beta}$	$\alpha = 2.79 \times 10^{-4} + 1.3 \times 10^{-4} \times RH$ $- 3.43 \times 10^{-6} \times RH^{2}$ $+ 7.52 \times 10^{-8} \times RH^{3}$ $\beta = 4 \times 10^{-2} \times (T-294) (T < 282K)$ $\beta = -0.48(T < 282 K)$	Evans and Jacob (2005)
	$\gamma_{N_2O_5,x} = \frac{1}{1+e^{-\lambda_x}}, = AB, AS, d;$ $\gamma_{N_2O_5,AB}^* = \min(\gamma_{N_2O_5,AB}, 0.08585)$ $\gamma_{N_2O_5,AS}^* = \min(\gamma_{N_2O_5,AS}, 0.053)$ $\gamma_{N_2O_5,d}^* = \min(\gamma_{N_2O_5,d}, 0.0124)$ Ammonium bisulfate (AB): $\lambda_{AB} = \beta_{10} + \beta_{11}RH_{46} + \beta_{12}T_{291}$ Ammonium sulfate (AS): $\lambda_{AS} = (\beta_{10} + \beta_{20}) + \beta_{11}RH_{46}$ (crystallizes at RH < 32.8%) Dry ammoniated sulfates: $\lambda_d = \beta_{d0} + \beta_{d1}RH + \beta_{d2}T_{293}$	$\beta_{10} = -2.67270$ $\beta_{20} = -0.97579$ $\beta_{11} = 0.09553$ $\beta_{12} = -0.20427$ $\beta_{d0} = -6.13376$ $\beta_{d1} = 0.03592$ $\beta_{d2} = -0.19688$ $T_{291} = \max(T - 291, 0)$ $T_{293} = \max(T - 293, 0)$ $RH_{46} = \min(RH - 46, 0)$	Davis et al. (2008), Appendix
Nitrate	$ \gamma_{N_2O_5,AN} = \frac{1}{1 + e^{-\lambda_{AN}}} \gamma_{N_2O_5,AN}^* = \min (\gamma_{N_2O_5,AN}, 0.0154) \lambda_{AN} = \beta_{30} + \beta_{31}RH $	$\beta_{30} = -8.10774$ $\beta_{31} = 0.04902$	Davis et al. (2008)
	$ \gamma_{N_2O_5} = \left(\frac{1}{\alpha} + \frac{c_{N_2O_5}S}{4K_HRTk_rV}\right)^{-1} k_{ref} = k_5\left(1 - \frac{k_a[NO_3]}{k_a[NO_3] + k_b[H_2O]}\right) $	V/S = 56 nm for Fig. 15 $k_{\text{ref}} = 5 \times 10^6 \text{ s}^{-1}$ $k_a/k_b = 30$	Griffith et al. (2009)
	$ \gamma_{N_2O_5} = Ak'(1 - \frac{1}{(\frac{k_B[H_2O]}{k_B[NO_3]}) + 1 + (\frac{k_C[CI^-]}{k_B[NO_3]})}) $ $ A = \frac{4V}{c_{N_2O_5}S} K_H $ $ k' = \beta - \beta e^{(-\delta[H_2O])} $	V/S = 37.5 nm for Fig. 15 $\beta = 1.15 \times 10^6 \text{s}^{-1}$ $\delta = 1.3 \times 10^{-1} \text{M}^{-1}$ $k_b/k_a = 6.0 \times 10^{-2}$ $k_c/k_a = 29$	Bertram and Thornton (2009)
Sulfate-nitrate	$\gamma_{\text{N}_2\text{O}_5,\text{mix}} = f \cdot \gamma_1 + (1 - f) \cdot \gamma_2$ $f = \frac{m_{\text{SO}_4}}{m_{\text{SO}_4} + m_{\text{NO}_3}}$	m [mass]	Riemer et al. (2003)
	$\gamma_{N_2O_5,aq} = x_{AB}\gamma_{N_2O_5,AB}^* + x_{AS}\gamma_{N_2O_5,AS}^* + x_{AN}\gamma_{N_2O_5,AN}^*$	$x_{AN} = 1 - (x_{AS} + x_{AN})$ $x_{AS} = \max(0, \min(1 - x_{AN}, \frac{[NH_4^+]}{[NO_3^-] + [SO_4^{2^-}]} - 1))$ $x_{AN} = \frac{[NO_3^-]}{[NO_3^-] + [SO_4^{2^-}]}$	Davis et al. (2008)
Organic carbon	$\gamma_{\text{N}_2\text{O}_5} = \text{RH} \times 5.2 \times 10^{-4} \text{ (RH} < 57\%)$ $\gamma_{\text{N}_2\text{O}_5} = 0.03 \text{ (RH} \ge 57\%)$		Evans and Jacob (2005)
Organic coating	$\frac{1}{\gamma_{N_2O_5}} = \frac{1}{\gamma_{N_2O_5,core}} + \frac{1}{\gamma_{N_2O_5,coat}}$ $\gamma_{N_2O_5,core} = \gamma_{N_2O_5,mix}$ $\gamma_{N_2O_5,coat} = \frac{4RTH_{org}D_{org}R_c}{c_{N_2O_5}\ell R_p}$	$\begin{split} &H_{org}D_{org} = 0.03H_{aq}D_{aq} \\ &H_{aq} = 5000 \text{ moles m}^{-1} \text{ atm}^{-1} \\ &D_{aq} = &10^{-9} \text{ m}^2 \text{ s}^{-1} \end{split}$	Anttila et al. (2006), Riemer et al. (2009)
Black carbon	$\gamma_{\rm N_2O_5}=0.005$		Evans and Jacob (2005)
Sea salt	$ \gamma_{N_2O_5} = 0.005 \text{ (RH } < 62\%) $ $ \gamma_{N_2O_5} = 0.03 \text{ (RH } \ge 62\%) $		Evans and Jacob (2005)
Dust	$\gamma_{\rm N_2O_5}=0.01$		Evans and Jacob (2005)

as shown in Figure 15(top). The resulting $\gamma_{N_2O_5}$ function for sulfates at RH above 50% agrees well with the constant value of 0.02 suggested by Riemer et al. (2003) at 298 K. For dry ammoniated sulfate particles, a less RH-dependent $\gamma_{N_2O_5}$ function is recommended (Davis et al. 2008), and since the function does not surpass the upper limit of the experimental values even at high RH, no "alternative" parameterizations are necessary.

The parameterization of $\gamma_{\rm N_2O_5}$ by Davis and coworkers on nitrate particles is also RH dependent, but no apparent temperature dependence was observed. It covers a range from 0.0005 (RH = 10%) to 0.0145 (RH = 80%). The constant value of 0.002 proposed by Riemer et al. (2003) only corresponds to the $\gamma_{\rm N_2O_5}$ function by Davis et al. (2008) at 50% RH. Brown et al. (2009) compared these various parameterizations with field-based determinations of $\gamma_{\rm N_2O_5}$. These field-based determinations yielded $\gamma_{\rm N_2O_5}$ in the range of 0.5–6 × 10⁻³, which is substantially smaller than current parameterizations used for atmospheric modeling (Riemer et al. 2003; Evans and Jacob 2005; Davis et al. 2008). Moreover, a dependence of $\gamma_{\rm N_2O_5}$ on variables such as RH and aerosol composition was not apparent in the determinations.

The coating of particles by organic material also inhibits N_2O_5 uptake (Anttila et al. 2006) and has been suggested as a possible explanation for field observations of suppressed N_2O_5 uptake (Brown et al. 2006b). To quantify the effect of organic coatings, Anttila et al. (2006) treated the reactive uptake of gaseous N_2O_5 by aerosols using a resistor model. Their study considered coatings that are thick enough to be considered bulk absorbing phases, in contrast to monolayers or submonolayers that had been investigated previously. Anttila et al. (2006) presented the reaction probability in the form of

$$\gamma_{\text{N}_2\text{O}_5,\text{coat}} = \frac{4RTH_{\text{org}}D_{\text{org}}R_{\text{c}}}{c_{\text{N}_2\text{O}_5}\ell R_{\text{p}}},$$
 [7]

where R is the universal gas constant, T is the temperature, $H_{\rm org}$ is the Henry constant of the organic material, and $D_{\rm org}$ is the diffusion coefficient of the organic material; $R_{\rm p}$, $R_{\rm c}$, and ℓ are the radius of the particle, the radius of the core, and the thickness of the coating, respectively. As expected, the thicker the coating, the smaller the uptake of N_2O_5 by the particle. All the recommended values for constant variables are summarized in Table 2.

Combining both the nitrate- and organic-coating effects, Riemer et al. (2009) arrived at the following parameterization:

$$\frac{1}{\gamma_{N_2O_5}} = \frac{1}{\gamma_{N_2O_5,core}} + \frac{1}{\gamma_{N_2O_5,coat}}.$$
 [8]

In a 3-D model, Riemer et al. (2009) estimated the maximum effect of organic coatings by assuming that all available secondary organic material contributed to the coating. That analysis showed that organics could suppress N_2O_5 uptake significantly,

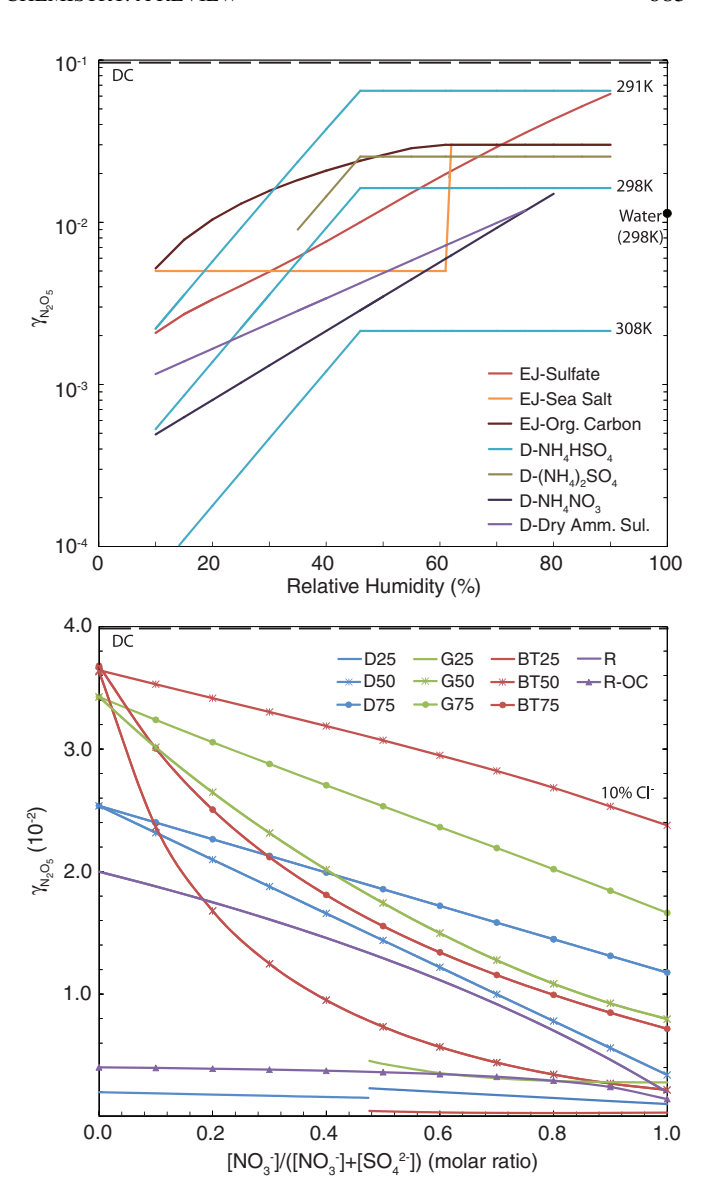


FIG. 15. N_2O_5 uptake reaction probability ($\gamma_{N_2O_5}$) parameterizations as a function of RH (top) and NO₃ content (bottom) recommended by DC-Dentener and Crutzen (1993), EJ-Evans and Jacob (2005), D-Davis et al. (2008), G-Griffiths et al. (2009), BT-Bertram and Thornton (2009), R-Riemer et al. (2003), and R-OC-Riemer et al. (2009). Temperature of 298 K is used for all temperature-dependent parameterizations, unless otherwise specified. RH values for [NO $_3$]-dependent $\gamma_{N_2O_5}$ parameterization (bottom) are indicated by the plot legend in percentage (e.g., D25 corresponds to 25% RH). The liquid water content of the aerosol, [H2O], for Griffiths et al. (2009) and Bertram and Thornton (2009) is calculated with the aerosol inorganics model (AIM, http://www.aim.env.uea.ac.uk/aim/aim.php). The crystallization relative humidity (CRH) is determined according to the recommendation given by Martin et al. (2003), below which the gamma values are omitted for Griffiths et al. (2009) and Bertram and Thornton (2009) parameterizations, and dry particle equation is used for Davis et al. (2008). [Cl-] is not taken into consideration for $\gamma_{N_2O_5}$ parameterization by Bertram and Thornton, except for one case (BT50) where 10% of the total molar anion concentrations ($[NO_3^-] + [SO_4^{2-}] + [Cl^-]$) is [Cl⁻] at 50% RH. For the organic-coating (OC) case (Riemer et al. 2009), particle size of 100 nm with 10% coating thickness is assumed. All parameterization constants used are summarized in Table 2. (Figure provided in color

reducing particle-phase nitrate concentrations by as much as 20%. They found the maximum effect of organics when nitrate concentrations are low and relatively little effect at high nitrate loadings. The parameterization by Riemer et al. (2009) leads to significantly lower reaction probabilities for N_2O_5 than the work presented by Davis et al. (2008).

A mechanistic parameterization of the nitrate effect in sulfate particles as a function of molar nitrate and water concentration was proposed by Griffiths et al. (2009),

$$k_{\rm r} = k_{\rm ref} \left(1 - \frac{k_{\rm a}[{\rm NO}_3^-]}{k_{\rm a}[{\rm NO}_3^-] + k_{\rm b}[{\rm H}_2{\rm O}]} \right),$$
 [9]

where $k_{\rm ref} = 5 \times 10^6 \, {\rm s}^{-1}$ and the ratio k_a to k_b is 30. The effective $\gamma_{\rm N_2O_5}$ for the proposed reaction constant, k_r , can be calculated by using the characteristic equation for reactive uptake coefficient on submicron aerosol when uptake is limited by the aerosol volume,

$$\gamma_{N_2O_5} = \left(\frac{1}{\alpha} + \frac{c_{N_2O_5}S}{4K_HRTk_rV}\right)^{-1},$$
[10]

where α is the mass accommodation coefficient, K_H is the Henry's law constant for N_2O_5 in water, R is the universal gas constant, and V is the aerosol volume. Their results also indicated a modest effect of dicarboxylic acids on uptake (see Section 2.1) and further confirm the strong influence of particle phase, liquid water content, and particulate nitrate concentration on N_2O_5 uptake rate.

Bertram and Thornton (2009) also proposed a mechanistic parameterization of $\gamma_{N_2O_5}$ that includes not only the competing effects of particle liquid water and nitrate but also chloride concentration,

$$\gamma_{N_2O_5} = Ak' \left(1 - \frac{1}{\left(\frac{k_b[H_2O]}{k_a[NO_3]}\right) + 1 + \left(\frac{k_c[CI^-]}{k_a[NO_3]}\right)} \right), \quad [11]$$

where A (3.2 × 10⁻⁸ s) is a constant that encompasses S, $c_{\rm N_2O_5}$, and $K_{\rm H}$, and k' can be calculated by using

$$k' = \beta - \beta e^{(-\delta[H_2O])}, \qquad [12]$$

with $\beta=1.15\times 10^6~{\rm s}^{-1}$ and $\delta=1.3\times 10^{-1}~{\rm M}^{-1}$. The ratios of k_b to k_a and k_c to k_a are 6.0×10^{-2} and 29, respectively. Their parameterization is based on measurements on mixed chloride–nitrate particles, and the authors found that the presence of chloride can offset the suppression of $\gamma_{\rm N_2O_5}$ due to nitrate. For aerosol that does not contain chloride, the parameterization by Bertram and Thornton (2009) is similar to the uptake reaction rate constant recommended by Griffiths et al. (2009), and their experimental results confirmed the dependence of $\gamma_{\rm N_2O_5}$ on competing particle water content

and nitrate. Investigations regarding the impact of these chemistry parameterizations on the regional or global scale are still in progress. All the major efforts to parameterize N_2O_5 uptake thus far are summarized in Table 3.

Regarding the dependence of $\gamma_{N_2O_5}$ on aerosol nitrate content, the various parameterizations compare as shown in Figure 15 (bottom). All parameterizations show a decrease of $\gamma_{N_2O_5}$ as the nitrate content increases. As described in Section 2.1, the decrease of γ_{N,O_5} is due to the fact that the recombination reaction $NO_2^+ + NO_3^-$ is favored when large nitrate concentrations are present. The RH-independent parameterization for N₂O₅ uptake inhibition by the nitrate effect recommended by Riemer et al. (2003) corresponds mostly closely with other RH-dependent parameterization at 50% RH (Davis et al. 2008; Griffiths et al. 2009; Bertram and Thornton 2009). The greatest variations in $\gamma_{N_2O_5}$ by increasing nitrate content in the particle are found in the mid-RH range. Bertram and Thornton (2009) also recommended the need for including chloride ion, and the parameterized function indicates that the presence of the halogen species offsets the influence of the nitrate effect (line labeled "10% Cl-").

The connection between N_2O_5 chemistry and the chlorine cycle has been investigated by Simon et al. (2009), using the Comprehensive Air quality Model with extensions (CAMx). They estimated the effects of observed nitryl chloride concentrations on local chemistry in southeast Texas and found that CINO_2 increases the total reactive chlorine mass by 20%-40% in this region; despite the high reactivity of chlorine, CINO_2 caused only modest increases in ozone concentrations.

There have also been models that treat the heterogeneous interaction between N₂O₅ and water in the troposphere as one involving only cloud water. Leaitch et al. (1988) studied the dissolution of N₂O₅ in cloud droplets by using a Lagrangian chemical model with winter conditions in northeastern region of the United States and compared the resulting NO₃⁻ content in cloud water with measured values. They showed that the mean production rate of HNO₃ via cloud scavenging is also much more efficient than homogeneous N₂O₅ hydrolysis, which was observed by Colvile et al. (1994) as well. The potential significance of N2O5 uptake on fog droplets was demonstrated through measurements by Wood et al. (2005), where the N₂O₅ mixing ratio was well below the detection limit of the instrument (LIF) during nights of high RH (above 70%). Osthoff et al. (2006) encountered similar conditions, where N₂O₅ mixing ratio falls below the detection limit in the presences of fog. Using $\gamma_{N_2O_5}$ = 0.04 on water droplet at 282 K (Vandoren et al. 1990), Sommariva et al. (2009) demonstrated that direct heterogeneous uptake of N₂O₅ by fog, when present, is the dominant atmospheric N₂O₅ loss pathway. The current IUPAC recommendation for heterogeneous N₂O₅ hydrolysis on water droplet has a negative temperature dependence,

$$\gamma_{\text{N}_2\text{O}_5} = 2.7 \times 10^{-5} \exp(1800/\text{T}).$$
 [13]

TABLE~3 Summary of major N_2O_5 heterogeneous reaction probability $(\gamma_{N_2O_5})$ parameterization studies

Reference	Characteristics	Comments
Dentener and Crutzen (1993)	Constant $\gamma_{N_2O_5} = 0.1$.	Generally over predicts N ₂ O ₅ uptake.
Riemer et al. (2003)	Mixed sulfate and nitrate parameterization.	Corresponds well with other RH and temperature-dependent parameterizations at 50% RH and 298 K.
Evans and Jacob (2005)	Categorized $\gamma_{N_2O_5}$ based upon aerosol composition: sulfate, organic carbon, black carbon, sea salt, and dust. $\gamma_{N_2O_5}$ for sulfate, organic carbon, and sea salt is functions of temperature and RH.	A wide range of aerosol types are considered.
Anttila et al. (2006)	Inhibition of aerosol uptake by organic coating is treated.	First to treat impact of organic coatings as a function of coating thickness and temperature.
Davis et al. (2008)	Rigorous statistical parameterization of $\gamma_{N_2O_5}$ as a function of the aerosol composition, RH, temperature, and phase state.	For inorganic aerosol, a wide range of temperature and RH are considered. Also, the phase of the particles is accounted.
Riemer et al. (2009)	Resistor model incorporating both mixed sulfate and nitrate parameterization (Riemer et al. 2003) and inhibition of aerosol uptake by organic coating (Anttila et al. 2006).	Comprehensive treatment of both inorganic species and organics. Nitrate and organics suppress $\gamma_{N_2O_3}$. Temperature and RH dependencies are not included.
Griffiths et al. (2009)	$\gamma_{N_2O_5}$ as a function of aerosol water and nitrate content.	On the basis of dicarboxylic-acids-containing sulfate aerosol experiments.
Bertram and Thornton (2009)	$\gamma_{\rm N_2O_5}$ as a function of aerosol water, nitrate, and chloride content.	On the basis of measurements on mixed chloride–nitrate particles.

5.2. Modeled Tropospheric N₂O₅ Profile Response to Other Trace Gases and Meteorological Conditions

As described in Section 4.2, the N₂O₅ vertical distribution tends to increase with altitude and often reaches a maximum near or at the top of the NBL. These profiles are the result of a complex interplay between chemical production and loss processes combined with the vertical transport of pollutants. Resolving these profiles adequately poses an important modeling issue, because pollutants in the NBL may not be well mixed, especially in rural areas (Fish et al. 1999). If the vertical model resolution is too coarse, the results may overestimate N₂O₅ levels near the surface and underestimate above the NBL (Galmarini et al. 1997). One must account for not only the chemical processes among trace gases but also prevailing meteorological conditions that govern the atmospheric stability. To quantify the altitude dependence of tropospheric N₂O₅ profiles, several investigators implemented gas-phase and heterogeneous reactions as well as meteorological conditions in 1-D models (Riemer et al. 2003, 2009; Gever and Stutz 2004).

Geyer and Stutz (2004) showed that the key factors controlling the N_2O_5 vertical gradient are surface NO emission strength and vertical gradients of VOC and particle surface area. Near the ground, when the simulated NO emissions are high,

available NO₃ at low altitudes undergoes titration and leads to a large indirect loss of N₂O₅. Vertical profiles of NO₃ are inversely related to the vertical gradient of VOC; the reaction between the two species reduces N₂O₅ levels in layers of the troposphere with high VOC concentrations. Depletion of NO₃ by NO and VOC, however, is balanced by the production of NO₃ via the reaction between NO₂ and O₃ (Riemer et al. 2003). N₂O₅ vertical profiles are positively correlated with NO₂, while negatively correlated with NO and VOC gradients. Figure 16 shows an example of calculated gas-phase vertical profiles for selected gas-phase species involved in N2O5 chemistry and illustrates the sensitivity of these profiles to atmospheric stability. The aerosol surface area gradient controls N₂O₅ levels directly by uptake through hydrolysis. While the reaction with NO is the dominant N₂O₅ loss pathway near the surface, at higher elevations, 20-80 m, the presence of high aerosol surfaces reduces the peak of N₂O₅ vertical profile in the NBL (Geyer and Stutz 2004). The reduced gradient in the N_2O_5 vertical profile in turn reduces the vertical transport of N₂O₅ to the surface layer. The role of aerosol surfaces on N₂O₅ profile is further complicated by the presence of nitrates and organic coatings on the aerosol that suppresses and inhibits the uptake of N₂O₅ on aerosols (Section 5.1).

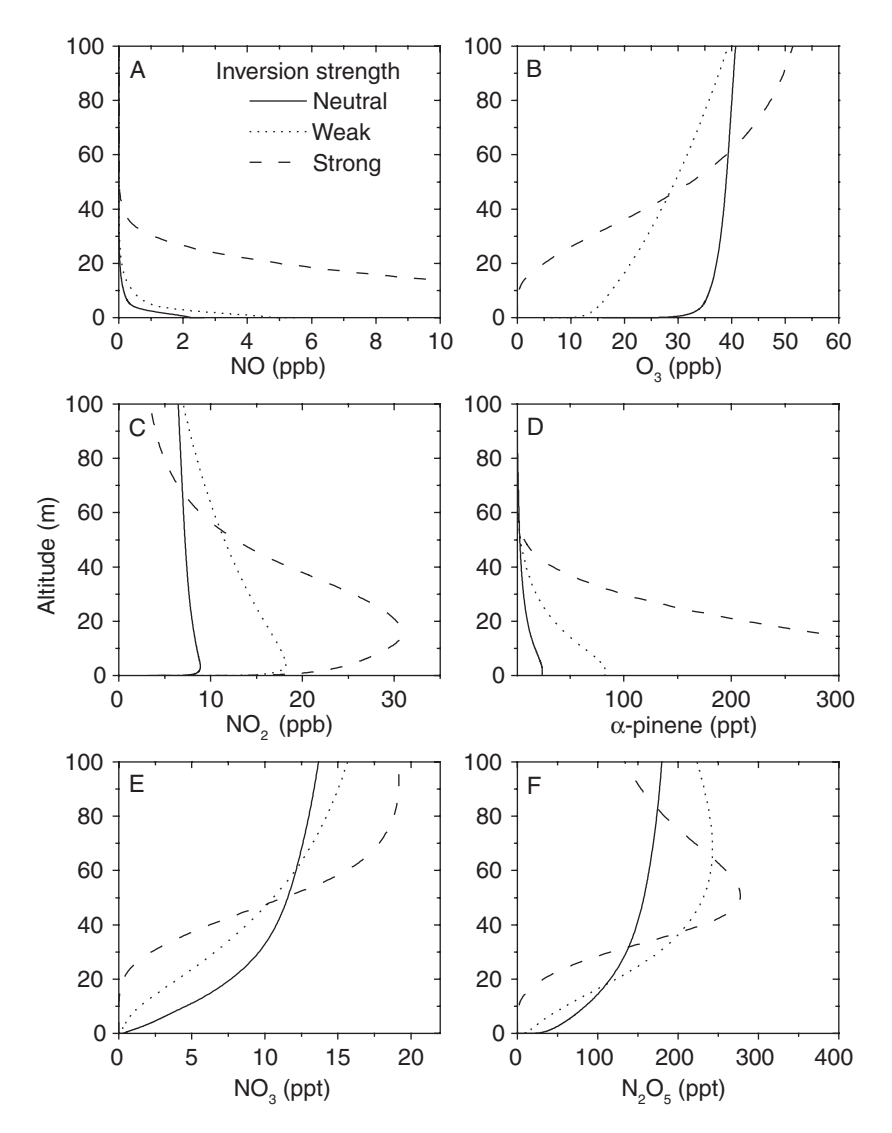


FIG. 16. Modeled NO, NO₂, NO₃, O₃, α -pinene, and N₂O₅ vertical profile responses to atmosphere stability (From Geyer and Stutz 2004).

Finally, numerical methods also present a source of uncertainty in simulating ambient N_2O_5 levels and spatial distributions. Though operator splitting in 3-D models is adequate for most tropospheric gaseous pollutants, it can be inadequate for fast-reacting species such as N_2O_5 (Nguyen and Dabdub 2003). Nguyen and Dabdub (2003) attributed N_2O_5 errors of as much as 44% to operator splitting. Nonoperator splitting methods avoid these errors, but their computational expense makes them impractical in most air quality model applications.

6. SUMMARY AND FUTURE RESEARCH NEEDS

Our understanding of the dynamics of N_2O_5 in the troposphere has improved significantly over the past few decades due to advances in laboratory measurements, ambient measurement techniques, and model developments. Although this review is not comprehensive with respect to the entire body of literature

on these areas, it provides (i) a review of the current understanding of the chemical mechanisms involving N_2O_5 formation and loss, along with its implications for atmospheric chemistry, (ii) a summary of the state-of-the-art measurement techniques available for making ambient in situ observations of N_2O_5 and the insights these measurements were able to provide, (iii) an examination of the uncertainties within the various methods of parameterization for multiphase/heterogeneous reactions of N_2O_5 , and (iv) an identification of areas in need of further exploration and research.

With respect to the last point, the following is a list of the outstanding questions that could be addressed by further laboratory, field, and model studies in the near future.

Laboratory Experiments

• In order to obtain a more comprehensive parameterization of $\gamma_{N_2O_5}$, measurements of the heterogeneous

- reaction probability under a wide range of relevant atmospheric conditions are needed. More specifically, the available literature lacks laboratory studies under conditions with low temperature and high RH.
- Detailed analysis of particles with mixed ice, sulfates, nitrates, chloride, and potentially other halide species requires closer examination.
- More research is needed on the distribution of the inorganic and organic phases in real atmospheric aerosol, along with a better-defined model parameterization of the potential effect of phase separation on N₂O₅ uptake coefficients.
- Further laboratory investigation of the third-order branch of the gas-phase reaction of N₂O₅ with water is required to resolve current discrepancies between laboratory and field determinations of the homogeneous reaction of N₂O₅ with water vapor.

Ambient Measurements

- Detailed understanding of the relative importance of N₂O₅ heterogeneous reaction on aerosols relative to other losses (e.g., indirect, oxidative NO₃ loss) should be determined from a larger body of field data that includes simultaneous measurements of N₂O₅, its precursors, VOC, and the physical and chemical properties of the aerosol, as well as meteorological parameters.
- \bullet The role of dry deposition as a loss process for N_2O_5 is poorly understood, especially in shallow surface layers and/or the nocturnal boundary layer. Further field studies examining vertical gradients in the lowest layers of the nocturnal boundary layer are needed.
- N₂O₅ chemistry is most prevalent in colder and darker periods of the year, where currently there is a smaller focus based on recent field studies. Understanding how N₂O₅ behaves in the winter season will be important to issues such as nitrate aerosol formation, global NO_x lifetimes and oxidant burdens, and halogen activation.
- Vertical profiles (e.g., from ground-based DOAS at various levels or from tall towers) and aircraft measurements of N₂O₅, related trace gases and aerosol within and above the NBL, and the overlying residual daytime boundary layer are needed to understand interactions between surface-level emissions, mixing, and chemistry that occurs aloft in the nighttime atmosphere.
- The existing database for simultaneous measurement of ClNO₂ and N₂O₅ remains too limited to accurately quantify the efficiency and extent of nighttime halogen activation.

Model Development

• There is the need for chemical transport models with high vertical resolutions that quantify the vertical transport of various trace gases and high horizontal resolutions that account for N_2O_5 production and destruction as a nonlinear function of NO_x concentration and sur-

- face area density. Model studies require vertical resolutions below 10 m in the nocturnal boundary layer, in particular near the ground, and several layers between 10 and 100 m. The description of vertical mixing in stable boundary layers remains a challenge and requires more research.
- In addition to the aerosol surface, the urban canopy can also provide the surface area for heterogeneous and surface reactions to occur in the urban environment. Chemical transport models currently do not consider this contribution.
- The more detailed the parameterizations become for γ_{N₂O₅}, the more assumptions need to be made regarding the aerosol mixing state, i.e., which fraction of the populations contains nitrate/chloride/organic coatings. This is a challenge for the representation of aerosol particles in chemical transport models.
- There is evidence from field measurements that the N₂O₅ hydrolysis on fog and cloud droplets could have a significant impact on the N₂O₅ budget. Modeling studies on this topic are rare but would help further our understanding in this regard, as measurement techniques have difficulties operating in cloudy or foggy environments.
- Model studies on ambient N₂O₅ profiles in the free troposphere, upper troposphere, and lower stratosphere are currently lacking. The sources of NO_x in this region are a major source of uncertainty, in particular the contribution of lightning-generated NO_x and the effect of its vertical distribution on the formation of N₂O₅.

Nomenclature

BBCEAS

ITCT

LED

LIF

MBL

Acronyms used in this article

formation

Light Emitting Diode

Marine Boundary Layer

Laser-Induced Fluorescence

	The state of the s
	troscopy
CEAS	Cavity-Enhanced Absorption Spectroscopy
CIMS	Chemical Ionization Mass Spectrometry
CRDS	Cavity Ring-Down Spectroscopy
cw	Continuous Wave
DMS	Dimethyl Sulfide
DOAS	Differential Optical Absorption Spectroscopy
DOY	Day of Year
GEOS	Goddard Earth Observing System
ICARTT	International Consortium for Atmospheric Re-
	search on Transport and Transformation
ICEALOT	International Chemistry Experiment in the Arc-
	tic LOwer Troposphere
ID	Ion Drift
IMR	Ion-Molecule Reaction Region

BroadBand Cavity Enhanced Absorption Spec-

Intercontinental Transport and Chemical Trans-

NBL Nighttime Boundary Layer NEAQS New England Air Quality Study

NOAA National Oceanic and Atmospheric Administra-

tion

OA Off-axis

PAN Peroxy Acteyl Nitrate

PMCAMx Particulate Matter Comprehensive Air Quality

Model with eXtensions

PSCRDS Phase Shift Cavity Ring-Down Spectroscopy

RH Relative Humidity

RHaMBLe Reactive Halogens in the Marine Boundary

Layer

SAPHIR TD Simulation of Atmospheric PHotochemistry In a

large Reaction Chamber

TD Thermal Dissociation
TexAQS Texas Air Quality Study
UTC Universal Time Coordinated
UW University of Washington
VOC Volatile Organic Compound

REFERENCES

Aldener, M., Brown, S. S., Stark, H., Williams, E. J., Lerner, B. M., Kuster, W. C., Goldan, P. D., Quinn, P. K., Bates, T. S., Fehsenfeld, F. C., and Ravishankara, A. R. (2006). Reactivity and Loss Mechanisms of NO₃ and N₂O₅ in a Polluted Marine Environment: Results from In Situ Measurements during New England Air Quality Study 2002. *J. Geophys. Res.* 111: D23S73.

Alexander, B., Hastings, M. G., Allman, D. J., Dachs, J., Thornton, J. A., and Kunasek, S. A. (2009). Quantifying Atmospheric Nitrate Formation Pathways Based on a Global Model of the Oxygen Isotopic Composition (Δ^{17} O) of Atmospheric Nitrate. *Atmos. Chem. Phys.* 9:5043–5056.

Allan, B. J., Carslaw, N., Coe, H., Burgess, R. A., and Plane, J. M. C. (1999). Observations of the Nitrate Radical in the Marine Boundary Layer. *J. Atmos. Chem.* 33:129–154.

Allan, B. J., McFiggans, G., Plane, J. M. C., Coe, H., and McFadyen, G. G. (2000). The Nitrate Radical in the Remote Marine Boundary Layer. J. Geophys. Res. 105:24191–124204.

Allan, W., Struthers, H., and Lowe, D. C. (2007). Methane Carbon Isotope Effects Caused by Atomic Chlorine in the Marine Boundary Layer: Global Model Results Compared with Southern Hemisphere Measurements. J. Geophys. Res. 112:D04306. doi: 04310.01029/02006JD007369.

Ambrose, J. L., Mao, H., Mayne, H. R., Stutz, J., Talbot, R., and Sive, B. C. (2007). Nighttime Nitrate Radical Chemistry at Appledore Island, Maine during the 2004 International Consortium for Atmospheric Research on Transport and Transformation. J. Geophys. Res. 112:D21302. doi: 10.1029/2007JD008756.

Anttila, T., Kiendler-Scharr, A., Tillmann, R., and Mentel, T. F. (2006). On the Reactive Uptake of Gaseous Compounds by Organic-Coated Aqueous Aerosols: Theoretical Analysis and Application to the Heterogeneous Hydrolysis of N₂O₅. J. Phys. Chem. A 110:10435–10443.

Apodaca, R. L., Dorn, H.-P., Brauers, T., Brown, S. S., Cohen, R. C., Crowley,
J. N., Dubé, W. P., Fry, J. L., Fuchs, H., Häseler, R., Kato, S., Kajii, Y.,
Kleffmann, J., KiendlerScharr, A., Labazan, I., Matsumoto, J., Nishida, S.,
Rohrer, F., Rollins, A. W., Schlosser, E., Schuster, G., Tillmann, R., Villena,
G., Wahner, A., Wegener, R., Wooldridge, P. J., and Simpson, W. R. (2011).
Intercomparison of N₂O₅ Sensors Using the SAPHIR Reaction Chamber.
Atmos. Chem. Phys. Discuss., in preparation.

Apodaca, R. L., Huff, D. M., and Simpson, W. R. (2008). The Role of Ice in N₂O₅ Heterogeneous Hydrolysis at High Latitudes. *Atmos. Chem. Phys.* 8:7451–7463. Asaf, D., Tas, E., Pedersen, D., Peleg, M., and Luria, M. (2010). Long-Term Measurements of NO₃ Radical at a Semiarid Urban Site: 2. Seasonal Trends and Loss Mechanisms. *Environ. Sci. Technol.* 44:5901–5907.

Atkinson, D. B. (2003). Solving Chemical Problems of Environmental Importance Using Cavity Ring-Down Spectroscopy. *Analyst* 128:117–125.

Atkinson, R., Baulch, D. L., Cox, R. A., Crowley, J. N., Hampson, R. F., Hynes, R. G., Jenkin, M. E., Rossi, M. J., and Troe, J. (2004). Evaluated Kinetic and Photochemical Data for Atmospheric Chemistry: Volume I—Gas Phase Reactions of O_X, HO_X, NO_X and SO_X Species. *Atmos. Chem. Phys.* 4:1461–1738

Atkinson, R., Winer, A. M., and Pitts, J. N. (1986). Estimation of Nighttime N₂O₅ Concentrations from Ambient NO₂ and NO₃ Radical Concentrations and the Role of N₂O₅ in Nighttime Chemistry. Atmos. Environ. 20:331–339.

Ayers, J. D., Apodaca, R. L., Simpson, W. R., and Baer, D. S. (2005). Off-Axis Cavity Ringdown Spectroscopy: Application to Atmospheric Nitrate Radical Detection. Appl. Optics 44(33):7239–7242.

Ayers, J. D., and Simpson, W. R. (2006). Measurements of N₂O₅ near Fairbanks, Alaska. J. Geophys. Res. 111:D14309.

Badger, C. L., Griffiths, P. T., George, I., Abbatt, J. P. D., and Cox, R. A. (2006). Reactive Uptake of N₂O₅ by Aerosol Particles Containing Mixtures of Humic Acid and Ammonium Sulfate. *J. Phys. Chem. A* 110:6986–6994.

Ball, S. M., and Jones, R. L. (2003). Broad-Band Cavity Ring-Down Spectroscopy. Chem. Rev. 103:5239–5262.

Ball, S. M., Langridge, J. M., and Jones, R. L. (2004). Broadband Cavity Enhanced Absorption Spectroscopy Using Light Emitting Diodes. *Chem. Phys. Lett.* 398:68–74.

Ball, S. M., Povey, I. M., Norton, E. G., and Jones, R. L. (2001). Broadband Cavity Ringdown Spectroscopy of the NO₃ Radical. *Chem. Phys. Lett.* 342:113–120.

Barnes, I., Becker, K. H., and Starcke, J. (1991). Fourier Transform Infrared Spectroscopic Observations of Gaseous Nitrosyl Iodine, Nitryl Iodine, and Iodine Nitrate. J. Phys. Chem. 95:9736–9740.

Bauer, S. E., Balkanski, Y., Schulz, M., and Hauglustaine, D. A. (2004). Global Modeling of Heterogeneous Chemistry on Mineral Aerosol Surfaces: Influence on Tropospheric Ozone Chemistry and Comparison to Observations. *J. Geophys. Res.* 109: D02304.

Bauer, S. E., Koch, D., Unger, N., Metzger, S. M., Shindell, D. T., and Streets, D. G. (2007). Nitrate Aerosols Today and in 2030: Importance Relative to Other Aerosol Species and Tropospheric Ozone. *Atmos. Chem. Phys.* 7:5043–5059.

Behnke, W., George, C., Scheer, V., and Zetzsch, C. (1997). Production and Decay of ClNO₂, from the Reaction of Gaseous N₂O₅ with NaCl Solution: Bulk and Aerosol Experiments. *J. Geophys. Res.-Atmos.* 102:3795–3804.

Bertram, T. H., and Thornton, J. A. (2009). Toward a General Parameterization of N₂O₅ Reactivity on Aqueous Particles: The Competing Effects of Particle Liquid Water, Nitrate and Chloride. *Atmos. Chem. Phys.* 9:8351–8363.

Bertram, T. H., Thornton, J. A., Riedel, T. P., Middlebrook, A. M., Bahreini, R., Bates, T. S., Quinn, P. K., and Coffman, D. J. (2009). Direct Observations of N₂O₅ Reactivity on Ambient Aerosol Particles. *Geophys. Res. Lett.* 36:L19803. doi: 10.1029/2009GL040248.

Bitter, M., Ball, S. M., Povey, I. M., and Jones, R. L. (2005). A Broadband Cavity Ringdown Spectrometer for In-Situ Measurements of Atmospheric Trace Gases. Atmos. Chem. Phys. 5:2547–2560.

Brown, S. S. (2003). Absorption Spectroscopy in High-Finesse Cavities for Atmospheric Studies. Chem. Rev. 103:5219–5238.

Brown, S. S., Dubé, W. P., Fuchs, H., Ryerson, T. B., Wollny, A. G., Brock, C.
A., Bahreini, R., Middlebrook, A. M., Neuman, J. A., Atlas, E., Roberts, J.
M., Osthoff, H. D., Trainer, M., Fehsenfeld, F. C., and Ravishankara, A. R.
(2009). Reactive Uptake Coefficients for N₂O₅ Determined from Aircraft Measurements during the Second Texas Air Quality Study: Comparison to Current Model Parameterizations. *J. Geophys. Res.* 114:D00F10. doi: 10.1029/2008JD011679.

- Brown, S. S., Dubé, W. P., Osthoff, H. D., Stutz, J., Ryerson, T. B., Wollny, A. G., Brock, C. A., Warneke, C., de Gouw, J. A., Atlas, E., Neuman, J. A., Holloway, J. S., Lerner, B. M., Williams, E. J., Kuster, W. C., Goldan, P. D., Angevine, W. M., Trainer, M., Fehsenfeld, F. C., and Ravishankara, A. R. (2007a). Vertical Profiles in NO₃ and N₂O₅ Measured from an Aircraft: Results from the NOAA P-3 and Surface Platforms during NEAQS 2004. *J. Geophys. Res.* 112:D22304. doi: 10.1029/2007JD008883.
- Brown, S. S., Dubé, W. P., Osthoff, H. D., Wolfe, D. E., Angevine, W. M., and Ravishankara, A. R. (2007b). High Resolution Vertical Distributions of NO₃ and N₂O₅ through the Nocturnal Boundary Layer. *Atmos. Chem. Phys.* 7:139–149.
- Brown, S. S., Neuman, J. A., Ryerson, T. B., Trainer, M., Dubé, W. P., Holloway,
 J. S., Warneke, C., de Gouw, J. A., Donnelly, S. G., Atlas, E., Matthew, B.,
 Middlebrook, A. M., Peltier, R., Weber, R. J., Stohl, A., Meagher, J. F.,
 Fehsenfeld, F. C., and Ravishankara, A. R. (2006a). Nocturnal Odd-Oxygen
 Budget and Its Implications for Ozone Loss in the Lower Troposphere.
 Geophys. Res. Lett. 33:L08801.
- Brown, S. S., Osthoff, H. D., Stark, H., Dubé, W. P., Ryerson, T. B., Warneke, C., de Gouw, J. A., Wollny, A. G., Parrish, D. D., Fehsenfeld, F. C., and Ravishankara, A. R. (2005). Aircraft Observations of Daytime NO₃ and N₂O₅ and Their Implications for Tropospheric Chemistry. *J. Photoc. Photobio. A* 176:270–278.
- Brown, S. S., Ryerson, T. B., Wollny, A. G., Brock, C. A., Peltier, R., Sullivan,
 A. P., Weber, R. J., Dubé, W. P., Trainer, M., Meagher, J. F., Fehsenfeld,
 F. C., and Ravishankara, A. R. (2006b). Variability in Nocturnal Nitrogen
 Oxide Processing and Its Role in Regional Air Quality. Science 311:67–70.
- Brown, S. S., Stark, H., Ciciora, S. J., McLaughlin, R. J., and Ravishankara, A. R. (2002). Simultaneous In Situ Detection of Atmospheric NO₃ and N₂O₅ via Cavity Ring-Down Spectroscopy. *Rev. Sci. Instrum.* 73:9. doi: 10.1063/1.1499214.
- Brown, S. S., Stark, H., Ciciora, S. J., and Ravishankara, A. R. (2001). In-Situ Measurement of Atmospheric NO₃ and N₂O₅ via Cavity Ring-Down Spectroscopy. *Geophys. Res. Lett.* 28:3227–3230.
- Brown, S. S., Stark, H., and Ravishankara, A. R. (2003a). Applicability of the Steady-State Approximation to the Interpretation of Atmospheric Observations of NO₃ and N₂O₅. *J. Geophys. Res.* 108:D174539.
- Brown, S. S., Stark, H., Ryerson, T. B., Williams, E. J., Nicks, D. K., Jr., Trainer, M., Fehsenfeld, F. C., and Ravishankara, A. R. (2003b). Nitrogen Oxides in the Nocturnal Boundary Layer: Simultaneous In Situ Measurements of NO₃, N₂O₅, NO₂, NO, and O₃. *J. Geophys. Res.* 108:D9, 4299. doi: 10.1029/2002JD002917.
- Busch, K. W., and Busch, M. A. (eds.) (1999). *Cavity-Ringdown Spectroscopy*. American Chemical Society, Washington, DC.
- Calvert, J. G. (1976). Hydrocarbon Involvement in Photochemical Smog Formation in Los-Angeles Atmosphere. *Environ. Sci. Technol.* 10:256– 262.
- Chang, J. S., Brost, R. A., Isaksen, I. S. A., Madronich, S., Middleton, P., Stockwell, W. R., and Walcek, C. J. (1987). A Three-Dimensional Eulerian Acid Deposition Model: Physical Concepts and Formulation. *J. Geophys. Res.* 92:14681–14700.
- Colvile, R. N., Choularton, T. W., Gallagher, M. W., Wicks, A. J., Downer, R. M., Tyler, B. J., Storeton-West, K. J., Fowler, D., Cape, J. N., Dollard, G. J., Davies, T. J., Jones, B. M. R., Penkett, S. A., Bandy, B. J., and Burgess, R. A. (1994). Observation on Great Dun Fell of the Pathways by Which Oxides of Nitrogen Are Converted to Nitrate. *Atmos. Environ.* 28:397–408.
- Cosman, L. M., and Bertram, A. K. (2008). Reactive Uptake of N_2O_5 on Aqueous H_2SO_4 Solutions Coated with 1-Component and 2-Component Monolayers. *J. Phys. Chem. A* 112:4625–4635.
- Cosman, L. M., Knopf, D. A., and Bertram, A. K. (2008). N₂O₅ Reactive Uptake on Aqueous Sulfuric Acid Solutions Coated with Branched and Straight-Chain Insoluble Organic Surfactants. *J. Phys. Chem. A* 112: 2386–2396.
- Crowley, J. N., Schuster, G., Pouvesle, N., Parchatka, U., Fischer, H., Bonn, B., Bingemer, H., and Lelieveld, J. (2010). Nocturnal Nitrogen Oxides at

- a Rural Mountain-Site in South-Western Germany. Atmos. Chem. Phys. 10:2795–2812.
- Crutzen, P. J. (1971). Ozone Production Rates in an Oxygen-Hydrogen-Nitrogen Oxide Atmosphere. J. Geophys. Res. 76:7311–7127.
- Davidson, J. A., Viggiano, A. A., Howard, C. J., Dotan, I., Fehsenfeld, F. C., Albritton, D. L., and Ferguson, E. E. (1978). Rate Constants for the Reactions of O₂⁺, NO₂⁺, NO⁺, H₃O⁺, CO₃⁻, NO₂⁻, and Halide Ions with N₂O₅ at 300 K. J. Chem. Phys. 68:2085–2087.
- Davis, J. M., Bhave, P. V., and Foley, K. M. (2008). Parameterization of N₂O₅ Reaction Probabilities on the Surface of Particles Containing Ammonium, Sulfate, and Nitrate. Atmos. Chem. Phys. 8:5295–5311.
- Dentener, F. J., and Crutzen, P. J. (1993). Reaction of N₂O₅ on Tropospheric Aerosols: Impact on the Global Distributions of NO_x, O₃, and OH. *J. Geo-phys. Res.* 98:7149–7163.
- Dimitroulopoulou, C., and Marsh, A. R. W. (1997). Modeling Studies of NO₃ Nighttime Chemistry and Its Effects on Subsequent Ozone Formation. *Atmos. Environ.* 31:3041–3157.
- Dubé, W. P., Brown, S. S., Osthoff, H. D., Nunley, M. R., Ciciora, S. J., Paris, M. W., McLaughlin, R. J., and Ravishankara, A. R. (2006). Aircraft Instrument for Simultaneous, In-Situ Measurements of NO₃ and N₂O₅ via Cavity Ring-Down Spectroscopy. *Rev. Sci. Instrum.* 77:034101. doi: 10.1063/1061.2176058.
- Emmerson, K. M., and Evans, M. J. (2009). Comparison of Tropospheric Gas-Phase Chemistry Schemes for Use within Global Models. *Atmos. Chem. Phys.* 9:1831–1845.
- Erickson, D. J., Seuzaret, C., Keene, W. C., and Gong, S. L. (1999). A General Circulation Model Based Calculation of HCl and ClNO₂ Production from Sea Salt Dechlorination: Reactive Chlorine Emissions Inventory. *J. Geophys. Res.-Atmos.* 104:8347–8372.
- Evans, M. J., and Jacob, D. J. (2005). Impact of New Laboratory Studies of N₂O₅ Hydrolysis on Global Model Budgets of Tropospheric Nitrogen Oxides, Ozone and OH. *Geophys. Res. Lett.* 32:L09813. doi: 10.1029/2005GL022469.
- Fehsenfeld, F. C., Ancellet, G., Bates, T. S., Goldstein, A. H., Hardesty, R. M., Honrath, R., Law, K., Lewis, A. C., Leaitch, R., McKeen, S. A., Meagher, J., Parrish, D. D., Pszenny, A. A. P., Russel, P. B., Schlager, H., Seinfeld, J. H., Talbot, R., and Zbinden, R. (2006). International Consortium for Atmospheric Research on Transport and Transformation (ICARTT): North America to Europe—Overview of the 2004 Summer Field Study. J. Geophys. Res. 111:D23S01. doi: 10.1029/2006JD007829.
- Fehsenfeld, F. C., Howard, C. J., and Schmeltekopf, A. L. (1975). Gas Phase Ion Chemistry of HNO₃. *J. Chem. Phys.* 63:2835–2842.
- Feng, Y., and Penner, J. E. (2007). Global Modeling of Nitrate and Ammonium: Interaction of Aerosols and Tropospheric Chemistry. J. Geophys. Res. 112:D01304. doi: 10.1029/2005JD006404.
- Fiedler, S. E., Hese, A., and Ruth, A. A. (2003). Incoherent Broad-Band Cavity-Enhanced Absorption Spectroscopy. *Chem. Phys. Lett.* 371:284– 294.
- Finlayson-Pitts, B. J., Ezell, M. J., and Pitts, J. N., Jr. (1989a). Formation of Chemically Active Compounds by Reactions of Atmospheric NaCl Particles with Gaseous N₂O₅ and ClNO₂. Nature 337:241–244.
- Finlayson-Pitts, B. J., Livingston, F. E., and Berko, H. N. (1989b). Synthesis and Identification by Infrared Spectroscopy of Gaseous Nitryl Bromide. J. Phys. Chem. 93:4397–4400.
- Fish, D. J., Shallcross, D. E., and Jones, R. L. (1999). The Vertical Distribution of NO₃ in the Atmospheric Boundary Layer. *Atmos. Environ.* 33:687–691
- Foley, K. M., Roselle, S. J., Appel, K. W., Bhave, P. V., Pleim, J. E., Otte, T. L., Mathur, R., Sarwar, G., Young, J. O., Gilliam, R. C., Nolte, C. G., Kelly, J. T., Gilliland, A. B., and Bash, J. O. (2010). Incremental Testing of the Community Multiscale Air Quality (CMAQ) Modeling System Version 4.7. Geosci. Model Dev. 3:205–226.
- Folkers, M. (2001). Bestimmung der reaktionswahrscheinlichkeit von N_2O_5 an troposhärisch relevanten aerosolen. PhD Thesis, Universität Köln.

- Folkers, M., Mentel, T. F., and Wahner, A. (2003). Influence of an Organic Coating on the Reactivity of Aqueous Aerosols Probed by the Heterogeneous Hydrolysis of N₂O₅. *Geophys. Res. Lett.* 30(12):1644.
- Fortner, E. C., Zhao, J., and Zhang, R. (2004). Development of Ion Drift-Chemical Ionization Mass Spectrometry. Anal. Chem. 76: 5436–5440.
- Fry, J. L., Kiendler-Scharr, A., Rollins, A. W., Wooldridge, P. J., Brown, S. S., Fuchs, H., Dubé, W. P., Mensah, A., dal Maso, M., Tillmann, R., Dorn, H.-P., Brauers, T., and Cohen, R. C. (2008). Organic Nitrate and Secondary Organic Aerosol Yield from NO₃ Oxidation of β-Pinene Evaluated Using a Gas-Phase Kinetics/Aerosol Partitioning Model. *Atmos. Chem. Phys.* 9:1431–1449.
- Fuchs, H., Ball, S. M., Bohn, B., Brauers, T., Cohen, R. C., Dorn, H.-P., Dubé, W. P., Fry, J. L., Häseler, R., Heitmann, U., Jones, R. L., Kleffmann, J., Mentel, T. F., Müsgen, P., Rohrer, F., Rollins, A. W., Ruth, A. A., Kiendler-Scharr, A., Schlosser, E., Shillings, A. J. L., Tillmann, R., Varma, R. M., Venables, D. S., Villena Tapia, G., Wahner, A., Wegener, R., Wooldridge, P. J., and Brown, S. S. (2010). Intercomparison of Measurements of NO₂ Concentrations in the Atmosphere Simulation Chamber SAPHIR during the NO3Comp Campaign. Atmos. Meas. Tech. 3:21–37.
- Fuchs, H., Dubé, W. P., Ciciora, S. J., and Brown, S. S. (2008). Determination of Inlet Transmission and Conversion Efficiencies for In Situ Measurements of the Nocturnal Nitrogen Oxides, NO₃, N₂O₅ and NO₂, via Pulsed Cavity Ring-Down Spectroscopy. *Anal. Chem.* 80:6010–6017. doi: 10.1021/ac8007253.
- Galmarini, S., Duynkerke, P. G., and Vila-Guerau de Arellano, J. (1997). Evolution of Nitrogen Oxide Chemistry in the Nocturnal Boundary Layer. J. Appl. Meteorol. 36:943–957.
- Geyer, A., Ackermann, R., Dubois, R., Lohrmann, B., Müller, T., and Platt, U. (2001). Long-Term Observation of Nitrate Radicals in the Continental Boundary Layer near Berlin. Atmos. Environ. 35:3619– 3631.
- Geyer, A., Alicke, B., Ackermann, R., Dubois, R., Martinez, M., Harder, H., Brune, W., di Carlo, P., Williams, E., Jobson, T., Hall, S., Shetter, R., and Stutz, J. (2003). Direct Observations of Daytime NO₃: Implications for Urban Boundary Layer Chemistry. J. Geophys. Res. 108:D4368. doi: 10.1029/2002JD002967.
- Geyer, A., and Stutz, J. (2004). Vertical Profiles of NO₃, N₂O₅, O₃, and NO_x in the Nocturnal Boundary Layer: 2. Model Studies on the Altitude Dependence of Composition and Chemistry. *J. Geophys. Res.* 109:D12307. doi: 10.1029/2003JD004211.
- Griffiths, P. T., Badger, C. L., Cox, R. A., Folkers, M., Henk, H. H., and Mentel, T. F. (2009). Reactive Uptake of N₂O₅ by Aerosols Containing Dicarboxylic Acids. Effect of Particle Phase, Composition, and Nitrate Content. *J. Phys. Chem. A* 113:5082–5090.
- Griffiths, P. T., and Cox, R. A. (2009). Temperature Dependence of Heterogeneous Uptake of N₂O₅ by Ammonium Sulfate Aerosol. *Atmos. Sci. Lett.* 10:159–163.
- Gross, S., and Bertram, A. K. (2008). Reactive Uptake of NO₃, N₂O₅, NO₂, HNO₃, and O₃ on Three Types of Polycyclic Aromatic Hydrocarbon Surfaces. *J. Phys. Chem. A* 112:3104–3113.
- Gross, S., and Bertram, A. K. (2009). Products and Kinetics of the Reactions of an Alkane Monolayer and a Terminal Alkene Monolayer with NO₃ Radicals. *J. Geophys. Res.-Atmos.* 114:D02307. doi: 10.1029/2008JD010987.
- Gross, S., Iannone, R., Xiao, S., and Bertram, A. K. (2009). Reactive Uptake Studies of NO₃ and N₂O₅ on Alkenoic Acid, Alkanoate, and Polyalcohol Substrates to Probe Nighttime Aerosol Chemistry. *Phys. Chem. Chem. Phys.* 11:7792–7803.
- Hallquist, M., Stewart, D. J., Stephenson, S. K., and Cox, R. A. (2003). Hydrolysis of N₂O₅ on Sub-Micron Sulfate Aerosols. *Phys. Chem. Chem. Phys.* 5:3453–3463
- Hanson, D. R., and Ravishankara, A. R. (1991). The Reaction Probabilities of CIONO₂ and N₂O₅ on Polar Stratospheric Cloud Materials. *J. Geophys. Res.* 96:5081–5091.

- Hanway, D., and Tao, F.-M. (1998). A Density Function Theory and Ab Initio Study of the Hydrolysis of Dinitrogen Pentoxide. *Chem. Phys. Lett.* 285:459–466.
- Harrison, M. A. J., Barra, S., Borghesi, D., Vione, D., Arsene, C., and Olariu, R. I. (2005). Nitrated Phenols in the Atmosphere: A Review. Atmos. Environ. 39:231–248.
- Heard, D. E., and Pilling, M. J. (2003). Measurement of OH and HO₂ in the Troposphere. *Chem. Rev.* 103:5163–5198.
- Hecht, T. A., and Seinfeld, J. H. (1972). Development and Validation of a Generalized Mechanism for Photochemical Smog. *Environ. Sci. Technol.* 6:47–57.
- Heikes, B. G., and Thompson, A. M. (1983). Effects of Heterogeneous Processes on NO₃, HONO, and HNO₃ Chemistry in the Troposphere. *J. Geophys. Res.* 88:10883–10895.
- Heintz, F., Platt, U., Flentje, H., and Dubois, R. (1996). Long-Term Observation of Nitrate Radicals at the Tor Station, Kap Arkona (Ruegen). J. Geophys. Res. 101(D17):22891–22910.
- Holland, F., Hessling, M., and Hofzumahaus, A. (1995). In Situ Measurement of Tropospheric OH Radicals by Laser-Induced Fluorescence—A Description of the Kfa Instrument. J. Atmos. Sci. 52(19):3393–3401.
- Horn, A. B., Koch, T., Chesters, M. A., McCoustra, M. R. S., and Sodeau, J. R. (1994). A Low-Temperature Infrared Study of the Reactions of the Stratospheric NO, Reservoir Species Dinitrogen Pentoxide with Water Ice, 80–160 K. J. Phys. Chem. 98:946–951.
- Hov, Ø., Eliassen, A., and Simpson, D. (1988). Calculations of the Distribution of NO_x Compounds in Europe, in *Tropospheric Ozone*, I. Isaksen, ed., D. Reidel, Norwell, MA, pp. 239–261.
- Hu, J. H., and Abbatt, J. P. D. (1997). Reaction Probabilities for N₂O₅ Hydrolysis on Sulfuric Acid and Ammonium Sulfate Aerosols at Room Temperature. *J. Phys. Chem. A* 101:871–878.
- Huey, L. G., Hanson, D. R., and Howard, C. J. (1995). Reactions of SF₆⁻ and I⁻ with Atmospheric Trace Gases. *J. Phys. Chem.* 99:5001–5008.
- IUPAC. (2010). Subcommittee for Gas Kinetic Data Evaluation. http://www.iupac-kinetic.ch.cam.ac.uk.
- Johnston, H. (1971). Reduction of Stratospheric Ozone by Nitrogen Oxide Catalysts from Supersonic Transport Exhaust. Science 173:517–522.
- Johnston, H., Davis, H. F., and Lee, Y. T. (1996). NO₃ Photolysis Product Channels: Quantum Yields from Observed Energy Thresholds. J. Phys. Chem. 100:4713–4723.
- Kane, S. M., Caloz, F., and Leu, M.-T. (2001). Heterogeneous Uptake of Gaseous N₂O₅ by (NH₄)₂SO₄, NH₄HSO₄, and H₂SO₄ Aerosols. *J. Phys. Chem. A*, 105:6465–6470.
- Karagulian, F., and Rossi, M. J. (2005). The Heterogeneous Chemical Kinetics of NO₃ on Atmospheric Mineral Dust Surrogates. *Phys. Chem. Chem. Phys.* 7:3150–3162.
- Karagulian, F., and Rossi, M. J. (2007). Heterogeneous Chemistry of the NO₃ Free Radical and N₂O₅ on Decane Flame Soot at Ambient Temperature: Reaction Products and Kinetics. J. Phys. Chem. A 111: 1914–1926.
- Karagulian, F., Santschi, C., and Rossi, M. J. (2006). The Heterogeneous Chemical Kinetics of N₂O₅ on CaCO₃ and Other Atmospheric Mineral Dust Surrogates. *Atmos. Chem. Phys.* 6:1373–1388.
- Karydis, V. A., Tsimpidi, A. P., and Pandis, S. N. (2007). Evaluation of a Three-Dimensional Chemical Transport Model (PMCAMx) in the Eastern United States for All Four Seasons. *J. Geophys. Res.* 112:D14211. doi: 10.1029/2006JD007890.
- Kercher, J. P., Riedel, T. P., and Thornton, J. A. (2009). Chlorine Activation by N₂O₅: Simultaneous, In-Situ Detection of ClNO₂ and N₂O₅ by Chemical Ionization Mass Spectrometry. *Atmos. Meas. Tech.* 2:193–204.
- King, M. D., Dick, E. M., and Simpson, W. R. (2000). A New Method for the Atmospheric Detection of the Nitrate Radical (NO₃). Atmos. Environ. 34:685–688.
- Langridge, J. M., Ball, S. M., and Jones, R. L. (2006). A Compact Broadband Cavity Enhanced Absorption Spectrometer for Detection

- of Atmospheric NO₂ Using Light Emitting Siodes. *Analyst* 131:916–922.
- Langridge, J. M., Ball, S. M., Shillings, A. J. L., and Jones, R. L. (2008).
 A Broadband Absorption Spectrometer Using Light Emitting Diodes for Ultrasensitive, In Situ Trace Gas Detection. *Rev. Sci. Instrum.* 79:1. doi: 10.1063/1.3046282.
- Leaitch, W. R., Bottenheim, J. W., and Strapp, J. W. (1988). Possible Contribution of N₂O₅ Scavenging to HNO₃ Observed in Winter Stratiform Cloud. *J. Geophys. Res.* 93:12569–12584.
- Lei, W., Zhang, R., Tie, X., and Hess, P. (2004). Chemical Characterization of Ozone Formation in the Houston-Galveston Area: A Chemical Transport Model Study. J. Geophys. Res., 109: D12301.
- Leu, M. T., Timonen, R. S., Keyser, L. F., and Yung, Y. L. (1995). Heterogeneous Reactions of $HNO_{3(g)}+NaCl_{(s)}\geq HCl_{(g)}+NaNO_{3(s)}$ and $N_2O_{5(g)}+NaCl_{(s)}\geq CINO2_{(g)}+NaNO_{3(s)}$. *J. Phys. Chem.* 99:13203–13212.
- Li, S.-M., Anlauf, K. G., and Wiebe, H. A. (1993). Heterogeneous Nighttime Production and Deposition of Particle Nitrate at a Rural Site in North America during Summer 1988. J. Geophys. Res. 98:5139–5157.
- Liao, H., and Seinfeld, J. H. (2005). Global Impacts of Gas-Phase Chemistry-Aerosol Interactions on Direct Radiative Forcing by Anthropogenic Aerosols and Ozone. J. Geophys. Res. 110:D18208. doi: 10.1029/2005JD005907.
- Lillis, D., Cruz, C. N., Collett, J., Jr., Richards, L. W., and Pandis, P. N. (1999).
 Production and Removal of Aerosol in a Polluted Fog Layer: Model Evaluation and Fog Effect on PM. Atmos. Environ. 33:4797–4816.
- Mak, J., Gross, S., and Bertram, A. K. (2007). Uptake of NO₃ on Soot and Pyrene Surfaces. *Geophys. Res. Lett.* 34:L10804. doi: 10.1029/2007GL029756.
- Martin, S. T., Schlenker, J. C., Malinowski, A., Hung, H.-M., and Rudich, Y. (2003). Crystallization of Atmospheric Sulfate-Nitrate-Ammonium Particles. *Geophys. Res. Lett.* 30:2102. doi: 10.1029/2003GL017930.
- Matsumoto, J., Imagawa, K., Imai, H., Kosugi, N., Ideguchi, M., Kato, S., and Kajii, Y. (2006). Nocturnal Sink of NO_x via NO₃ and N₂O₅ in the Outflow from a Source Area in Japan. *Atmos. Environ.* 40:6294–6302.
- Matsumoto, J., Imai, H., Kosugi, N., and Kajii, Y. (2005a). In Situ Measurement of N_2O_5 in the Urban Atmosphere by Thermal Decomposition/Laser-Induced Fluorescence Technique. *Atmos. Environ.* 39:6802–6811.
- Matsumoto, J., Kosugi, N., Imai, H., and Kajii, Y. (2005b). Development of a Measurement System for Nitrate Radical and Dinitrogen Pentoxide Using a Thermal Conversion/Laser-Induced Fluorescence Technique. Rev. Sci. Instrum. 76:064101.
- McLaren, R., Salmon, R. A., Liggio, J., Hayden, K. L., Anlauf, K. G., and Leaitch, W. R. (2004). Nighttime Chemistry at a Rural Site in the Lower Fraser Valley. Atmos. Environ. 38:5837–5848.
- McNeill, V. F., Patterson, J., Wolfe, G. M., and Thornton, J. A. (2006). The Effect of Varying Levels of Surfactant on the Reactive Uptake of N_2O_5 to Aqueous Aerosol. *Atmos. Chem. Phys.* 6:1635–1644.
- McNeill, V. F., Wolfe, G. M., and Thornton, J. A. (2007). The Oxidation of Oleate in Submicron Aqueous Salt Aerosols: Evidence of a Surface Process. *J. Phys. Chem. A* 111:1073–1083.
- Meinen, J., Thieser, J., Platt, U., and Leisner, T. (2010). Technical Note: Using a High Finesse Optical Resonator to Provide a Long Light Path for Differential Optical Absorption Spectroscopy: CE-DOAS. Atmos. Chem. Phys. 10:3901–3914.
- Mentel, T. F., Bleilebens, D., and Wahner, A. (1996). A Study of Nighttime Nitrogen Oxide Oxidation in a Large Reaction Chamber—The Fate of NO₂, N₂O₅, HNO₃, and O₃ at Different Humidities. *Atmos. Environ.* 30:4007–4020.
- Mentel, T. F., Sohn, M., and Wahner, A. (1999). Nitrate Effect in the Heterogeneous Hydrolysis of Dinitrogen Pentoxide on Aqueous Aerosols. *Phys. Chem. Phys.* 1:5451–5457.
- Moise, T., Talukdar, R. K., Frost, G. J., Fox, R. W., and Rudich, Y. (2002).Reactive Uptake of NO₃ by Liquid and Frozen Organics. J. Geophys. Res., 107: 4014.

- Morris, E. D., and Niki, H. (1973). Reaction of Dinitrogen Pentoxide with Water. J. Phys. Chem. 77:1929–1932.
- Mozurkewich, M., and Calvert, J. G. (1988). Reaction Probability of N₂O₅ on Aqueous Aerosols. J. Geophys. Res. 93:15889–15896.
- Nakayama, T., Ide, T., Taketani, F., Kawai, M., Takahashi, K., and Matsumi, Y. (2008). Nighttime Measurements of Ambient N₂O₅, NO₂, NO and O₃ in a Sub-Urban Area, Toyokawa, Japan. Atmos. Environ. 42: 1995–2006.
- Nguyen, K., and Dabdub, D. (2003). Development and Analysis of a Non-Splitting Solution for Three-Dimensional Air Quality Models. Atmos. Environ. 37:3741–3748. doi: 10.1016/S1352–2310(03)00348–0.
- O'Keefe, A., and Deacon, D. A. G. (1988). Cavity Ring-Down Optical Spectrometer for Absorption Measurements Using Pulsed Laser Sources. *Rev. Sci. Instrum.* 59:2544. doi: 10.1063/1.1139895.
- O'Keefe, A., and Lee, O. (1989). Trace Gas Analysis by Pulsed Laser Absorption Spectroscopy. Am. Lab. 21:19–22.
- Osthoff, H. D., Pilling, M. J., Ravishankara, A. R., and Brown, S. S. (2007). Temperature Dependence of the NO₃ Absorption Cross-Section above 298 K and Determination of the Equilibrium Constant for NO₃ + NO₂ → N₂O₅ at Atmospherically Relevant Conditions. *Phys. Chem. Chem. Phys.* 9:5785–5793. doi: 10.1039/b709193a.
- Osthoff, H. D., Roberts, J. M., Ravishankara, A. R., Williams, E. J., Lerner, B. M., Sommariva, R., Bates, T. S., Coffman, D., Quinn, P. K., Dibbs, J. E., Stark, H., Burkholder, J. B., Talukdar, R. K., Meagher, J. F., Fehsenfeld, F. C., and Brown, S. S. (2008). High Levels of Nitryl Chloride in the Polluted Subtropical Marine Boundary Layer. *Nat. Geosci.* 1:324–328.
- Osthoff, H. D., Sommariva, R., Baynard, T., Pettersson, A., Williams, E. J., Lerner, B. M., Roberts, J. M., Stark, H., Goldan, P. D., Kuster, W. C., Bates, T. S., Coffman, D., Ravishankara, A. R., and Brown, S. S. (2006). Observations of Daytime N₂O₅ in the Marine Boundary Layer during New England Air Quality Study—Intercontinental Transport and Chemical Transformation 2004. J. Geophys. Res. 111:D23S14. doi: 10.1029/2006JD007593.
- Park, S.-C., Burden, D. K., and Nathanson, G. M. (2007). The Inhibition of N₂O₅ Hydrolysis in Sulfuric Acid by 1-Butanol and 1-Hexanol Surfactant Coatings. J. Phys. Chem. A 111:2921–2929.
- Parrish, D. D., Allen, D. T., Bates, T. S., Estes, M., Fehsenfeld, F. C., Feingold, G., Ferrare, R., Hardesty, R. M., Meagher, J. F., Nielsen-Gammon, J., Pierce, R. B., Ryerson, T. B., Seinfeld, J. H., and Williams, E. J. (2008). Overview of the Second Texas Air Quality Study (TexAQS II) and the Gulf of Mexico Atmospheric Composition and Climate Study (GoMACCS). J. Geophys. Res. 114:D00F13. doi: 10.1029/2009JD011842.
- Patris, N., Cliff, S. S., Quinn, P. K., Kasem, M., and Thiemens, M. H. (2007). Isotopic Analysis of Aerosol Sulfate and Nitrate during ITCT-2k2: Determination of Different Formation Pathways as a Function of Particle Size. J. Geophys. Res., 112: D23301.
- Perner, D., Schmeltekopf, A., Winkler, R. H., Johnston, H. S., Calvert, J. G., Cantrell, C. A., and Stockwell, W. R. (1985). A Laboratory and Field Study of the Equilibrium N₂O₅ Yields Reversibly NO₃ + NO₂. J. Geophys. Res. 20:3807–3812.
- Platt, U., Allan, W., and Lowe, D. (2004). Hemispheric Average Cl Atom Concentration from ¹³C/¹²C Ratios in Atmospheric Methane. *Atmos. Chem. Phys.* 4:2393–2399.
- Platt, U., Meinen, J., Pöhler, D., and Leisner, T. (2009). Broadband Cavity Enhanced Differential Optical Absorption Spectroscopy (CE-DOAS)—Applicability and Corrections. Atmos. Meas. Tech. 2:713–723.
- Platt, U., Perner, D., Winer, A. M., Harris, G. W., and Pitts, J. N., Jr. (1980). Detection of NO₃ in the Polluted Troposphere by Differential Optical Absorption. *Geophys. Res. Lett.* 7:89–92.
- Platt, U., and Stutz, J. (2008). Differential Optical Absorption Spectroscopy Principles and Applications. Springer Berlin Heidelberg, New York.
- Pleim, J. E., Binkowski, F. S., Ching, J. K. S., Dennis, R. L., and Gallani, N. V. (1995). An Improved Representation of the Reaction of N₂O₅ on Aerosols for Mesoscale Air Quality Models, in Regional Photochemical Measurement and Modeling Studies, Vol 2—Results and Status of Modeling, A. J. Ranzieri

and P. A. Solomon, eds., A WMA International Speciality Conference, San Diego, CA. pp. 904–913.

- Raff, J. D., Njegic, B., Chang, W. L., Gordon, M. S., Dabdub, D., Gerber, R. B., and Finlayson-Pitts, B. J. (2009). Chlorine Activation Indoors and Outdoors via Surface-Mediated Reactions of Nitrogen Oxides with Hydrogen Chloride. P. Natl. A. Sci. USA 106:13647–13654.
- Riemer, N., Vogel, H., Vogel, B., Anttila, T., Mentel, T. F., Kiendler-Scharr, A. (2009). The Relative Importance of Organic Coatings for the Heterogeneous Hydrolysis of N₂O₅. J. Geophys. Res. 114:D17307. doi: 10.1029/2008JD011369.
- Riemer, N., Vogel, H., Vogel, B., Schell, B., Ackermann, I., Kessler, C., and Hass, H. (2003). Impact of the Heterogeneous Hydrolysis of N₂O₅ on Chemistry and Nitrate Aerosol Formation in the Lower Troposphere under Photosmog Conditions. J. Geophys. Res. 108:4144.
- Roberts, J. M., Osthoff, H. D., Brown, S. S., and Ravishankara, A. R. (2008). N₂O₅ Oxidizes Chloride to Cl₂ in Acidic Atmospheric Aerosol. *Science* 321:1059.
- Roberts, J. M., Osthoff, H. D., Brown, S. S., Ravishankara, A. R., Coffman, D., Quinn, P., and Bates, T. (2009). Laboratory Studies of Products of N₂O₅ Uptake on Cl⁻ Containing Substrates. *Geophys. Res. Lett.* 36:L20808. doi: 10.1029/2009GL0404448.
- Rollins, A. W., Kiendler-Scharr, A., Fry, J. L., Brauers, T., Brown, S. S., Dorn, H.-P., Dubé, W. P., Fuchs, H., Mensah, A., Mentel, T. F., Rohrer, F., Tilmann, R., Wegener, R., Wooldridge, P. J., and Cohen, R. C. (2009). Isoprene Oxidation by Nitrate Radical: Alkyl Nitrate and Secondary Organic Aerosol Yields. Atmos. Chem. Phys. 9:6685–6703.
- Russell, A. G., and Cass, G. R. (1986). Verification of a Mathematical Model for Aerosol Nitrate and Nitric Acid Formation and Its Use for Control Measure Evaluation. Atmos. Environ. 20:2011–2025.
- Russell, A. G., McRae, G. J., and Cass, G. R. (1985). The Dynamics of Nitric Acid Production and the Fate of Nitrogen Oxides. Atmos. Environ. 19:893–903.
- Saathoff, H., Naumann, K.-H., Riemer, N., Kamm, S., Möhler, O., Schurath, U., Vogel, H., and Vogel, B. (2001). The Loss of NO₂, HNO₃, NO₃/N₂O₅, and HO₂/HOONO₂ on Soot Aerosol: A Chamber and Modeling Study. *Geophys. Res. Lett.* 28:1957–1960. doi: 10.1029/2000GL012619.
- Sander, S. P., Friedl, R. R., Ravishankara, A. R., Golden, D. M., Kolb, C. E., Kurylo, M. J., Molina, M. J., Moortgat, G. K., Keller-Rudek, H., Finlayson-Pitts, B. J., Wine, P. H., Huie, R. E., and Orkin, V. L. (2006). Chemical Kinetics and Photochemical Data for Use in Atmospheric Studies, Evaluation Number 15. NASA/JPL Publication 06-2, Pasadena, CA.
- Schuster, G., Labazan, I., and Crowley, J. N. (2009). A Cavity Ring Down/Cavity Enhanced Absorption Device for Measurement of Ambient NO₃ and N₂O₅. Atmos. Meas. Tech. 2:1–13.
- Schwartz, S. E. (1986). Mass-Transport Considerations Pertinent to Aqueous Phase Reactions of Gases in Liquid Water Clouds, in *Chemistry of Multiphase Atmospheric System, NATO ASI Ser., Ser. G*, W. Jaeschke, ed., Springer-Verlag, New York, pp. 415–471.
- Schweitzer, F., Mirabel, P., and George, C. (1998). Multiphase Chemistry of N₂O₅, ClNO₂, and BrNO₂. J. Phys. Chem. A 102:3942–3952.
- Seisel, S., Borensen, C., Vogt, R., and Zellner, R. (2005). Kinetics and Mechanism of the Uptake of N₂O₅ on Mineral Dust at 298 K. Atmos. Chem. Phys. 5:3423–3432.
- Simon, H., Kimura, Y., McGaughney, G., Allen, D. T., Brown, S. S., Osthoff, H. D., Roberts, J. M., Byun, D., and Lee, D. (2009). Modeling the Impact of ClNO₂ on Ozone Formation in the Houston Area. *J. Geophys. Res.* 114:D00F03.
- Simpson, W. R. (2003). Continuous Wave Cavity Ring-Down Spectroscopy Applied to In Situ Detection of Dinitrogen Pentoxide (N₂O₅). Rev. Sci. Instrum. 74:7. doi: 10.1063/1.1578705
- Slusher, D. L., Huey, L. G., Tanner, D. J., Flocke, F., and Roberts, J. M. (2004). A Thermal Dissociation—Chemical Ionization Mass Spectrometry (TD-CIMS) Technique for the Simultaneous Measurement of Perox-

- yacetyl Radicals and Dinitrogen Pentoxide. J. Geophys. Res. 109:D19315. doi: 10.1029/2004JD004670
- Sommariva, R., Osthoff, H. D., Brown, S. S., Bates, T. S., Baynard, T., Coffman, D., de Gouw, J. A., Goldan, P. D., Kuster, W. C., Lerner, B. M., Stark, H., Warneke, C., Williams, E. J., Fehsenfeld, F. C., Ravishankara, A. R., and Trainer, M. (2009). Radicals in the Marine Boundary Layer during NEAQS 2004: A Model Study of Day-Time and Night-Time Sources and Sinks. Atmos. Chem. Phys. 9:3075–3093.
- Sommariva, R., Pilling, M. J., Bloss, W. J., Heard, D. E., Lee, J. D., Fleming, Z. L., Monks, P. S., Plane, J. M. C., Saiz-Lopez, A., Ball, S. M., Bitter, M., Jones, R. L., Brough, N., Penkett, S. A., Hopkins, J. R., Lewis, A. C., and Read, K. A. (2007). Night-Time Radical Chemistry during the NAMBLEX Campaign. Atmos. Chem. Phys. 7:587–598.
- Stelson, A. W., and Seinfeld, J. H. (1982). Relative Humidity and Temperature Dependence of the Ammonium Nitrate Dissociation Constant. Atmos. Environ. 16:983–992.
- Stewart, D. J., Griffiths, P. T., and Cox, R. A. (2004). Reactive Uptake Coefficients for Heterogeneous Reaction of N₂O₅ with Submicron Aerosols of NaCl and Natural Sea Salt. Atmos. Chem. Phys. 4:1381–1388.
- Stutz, J., Alicke, B., Ackermann, R., Geyer, A., White, A., and Williams, E. (2004). Vertical Profiles of NO₃, N₂O₅, O₃, and NO_x in the Nocturnal Boundary Layer: 1. Observations during the Texas Air Quality Study 2000. *J. Geophys. Res.* 109:D12306. doi: 10.1029/2003JD004209
- Stutz, J., Wong, K. W., Lawrence, L., Ziemba, L., Flynn, J. H., Rappenglück, B., and Lefer, B. (2009). Nocturnal NO₃ Radical Chemistry in Houston, TX. Atmos. Environ. 44:4099–4106
- Tang, M. J., Thieser, J., Schuster, G., and Crowley, J. N. (2010). Uptake of NO₃ and N₂O₅ to Saharan Dust, Ambient Urban Aerosol and Soot: A Relative Rate Study. Atmos. Chem. Phys. 10:2965–2974. doi: 10.5194/acp-10-2965-2010
- Thornton, J. A., and Abbatt, J. P. D. (2005). N₂O₅ Reaction on Submicron Sea Salt Aerosol: Kinetics, Products, and the Effect of Surface Active Organics. *J. Phys. Chem. A* 109:10004–10012.
- Thornton, J. A., Braban, C. F., and Abbatt, J. P. D. (2003). N₂O₅ Hydrolysis on Sub-Micron Organic Aerosol: The Effect of Relative Humidity, Particle Phase and Particle Size. *Phys. Chem. Chem. Phys.* 5(20):4593–4603.
- Thornton, J. A., Kercher, J. P., Riedel, T. P., Wagner, N. L., Cozic, J., Holloway, J. S., Dubé, W. P., Wolfe, G. M., Quinn, P. K., Alexander, B., and Brown, S. S. (2010). A Large Atomic Chlorine Source Inferred from Mid-Continental Reactive Nitrogen Chemistry. *Nature* 464:271–274.
- Thornton, J. A., Wooldrige, P. J., and Cohen, R. J. (2000). Atmospheric NO₂: In Situ Laser-Induced Fluorescence Detection at Parts per Trillion Mixing Ratios. Anal. Chem. 72:528–539.
- Tie, X., Brasseur, G., Emmons, L., Horowitz, L., and Kinnison, D. (2001).
 Effects of Aerosols on Tropospheric Oxidants: A Global Model Study. J. Geophys. Res. 106:22931–22964.
- Tie, X., Emmons, L., Horowitz, L., Brasseur, G., Ridley, B., Atlas, E., Stround, C., Hess, P., Klonecki, A., Madronich, S., Talbot, R., and Dibb, J. (2003). Effect of Sulfate Aerosol on Tropospheric NO_x and Ozone Budgets: Model Simulations and TOPSE Evidence. *J. Geophys. Res.* 108(D4):8364. doi: 10.1029/2001JD001508
- Tolbert, M. A., Rossi, M. J., and Golden, D. M. (1988). Antarctic Ozone Depletion Chemistry: Reactions of N₂O₅ with H₂O and HCl on Ice Surfaces. Science 240:1018–1021.
- Vandoren, J. M., Watson, L. R., Davidovits, P., Worsnop, D. R., Zahniser, M. S., and Kolb, C. E. (1990). Temperature-Dependence of the Uptake Coefficients of HNO₃, HCl, and N₂O₅ by Water Droplets. *J. Phys. Chem.* 94: 3265–3269.
- Varma, R. M., Venables, D. S., Ruth, A. A., Heitmann, U., Schlosser, E., and Dixneuf, S. (2009). Long Optical Cavities for Open-Path Monitoring of Atmospheric Trace Gases and Aerosol Extinction. Appl. Opt. 48: B150–B171.
- Venables, D. S., Gherman, T., Orphal, J., Wenger, J. C., and Ruth, A. A. (2006). High Sensitivity In Situ Monitoring of NO₃ in an Atmospheric

- Simulation Chamber Using Incoherent Broadband Cavity Enhanced Absorption Spectroscopy. *Environ. Sci. Technol.* 40:6758–6763.
- Voegele, A. F., Tautermann, C. S., Loerting, T., and Liedl, K. R. (2003). Toward Elimination of Discrepancies between Theory and Experiment: The Gas-Phase Reaction of N₂O₅ with H₂O. *Phys. Chem. Chem. Phys.* 5:487–495.
- von Friedeburg, C., Wagner, T., Geyer, A., Kaiser, N., Vogel, B., Vogel, H., and Platt, U. (2002). Derivation of Tropospheric NO₃ Profiles Using Off-Axis Differential Optical Absorption Spectroscopy Measurements during Sunrise and Comparison with Simulations. *J. Geophys. Res.* 107(D13):4168. doi: 10.1029/2001JD000481
- Vrekoussis, M., Mihalopoulos, N., Gerasopoulos, E., Kanakidou, M., Crutzen, P. J., and Lelieveld, J. (2007). Two-Years of NO₃ Radical Observations in the Boundary Layer over the Eastern Mediterranean. *Atmos. Chem. Phys.* 7:315–327.
- Wagner, C., Hanisch, F., Holmes, N., de Coninck, H., Schuster, G., and Crowley, J. N. (2008). The Interaction of N₂O₅ with Mineral Dust: Aerosol Flow Tube and Knudsen Reactor Studies. *Atmos. Chem. Phys.* 8:91–109.
- Wagner, C., Schuster, G., and Crowley, J. N. (2009). An Aerosol Flow Tube Study of the Interaction of N_2O_5 with Calcite, Arizona Dust and Quartz. *Atmos. Environ.* 43:5001–5008.
- Wahner, A., Mentel, T. F., Sohn, M., and Stier, J. (1998a). Gas-Phase Reaction of N₂O₅ with Water Vapor: Importance of Heterogeneous Hydrolysis of N₂O₅ and Surface Desorption of HNO₃ in a Large Teflon Chamber. *Geophys. Res.* Lett. 25:2169–2172.

- Wahner, A., Mentel, T. F., Sohn, M., and Stier, J. (1998b). Heterogeneous Reaction of N₂O₅ on Sodium Nitrate Aerosol. *J. Geophys. Res.* 103:31103–31112.
- Wang, S., Ackermann, R., and Stutz, J. (2006). Vertical Profiles of O₃ and NO_x Chemistry in the Polluted Nocturnal Boundary Layer in Phoenix, AZ: I. Field Observations by Long-Path DOAS. *Atmos. Chem. Phys.* 6:2671–2693.
- Wayne, R. P., Barnes, I., Biggs, P., Burrows, J. P., Canosamas, C. E., Hjorth, J., Lebras, G., Moortgat, G. K., Perner, D., Poulet, G., Restelli, G., and Sidebottom, H. (1991). The Nitrate Radical—Physics, Chemistry, and the Atmosphere. Atmos. Environ. A 25:1–203.
- Wood, E. C., Bertram, T. H., Wooldridge, P. J., and Cohen, R. C. (2005). Measurements of N₂O₅, NO₂, and O₃ East of the San Francisco Bay. *Atmos. Chem. Phys.* 5:483–491.
- Wood, E. C., Wooldridge, P. J., Freese, J. H., Albrecht, T., and Cohen, R. C. (2003). Prototype for In Situ Detection of Atmospheric NO₃ and N₂O₅ via Laser-Induced Fluorescence. *Environ. Sci. Technol.* 37(24):5732–5738.
- Yu, S., Dennis, R., Roselle, S., Nenes, A., Walker, J., Eder, B., Schere, K., and Swall, J. (2005). An Assessment of the Ability of 3-D Air Quality Models with Current Thermodynamic Equilibrium Models to Predict Aerosol NO₃⁻. J. Geophys. Res. 110:D07S13.
- Zheng, J., Zhang, R., Fortner, E. C., Volkamer, R. M., Molina, L., Aiken, A. C., Jimenez, J. L., Gaeggeler, K., Dommen, J., Dusanter, S., Stevens, P. S., and Tie, X. (2008). Measurements of HNO₃ and N₂O₅ Using Ion Drift-Chemical Ionization Mass Spectrometry during the MILAGRO/MCMA-2006 Campaign. Atmos. Chem. Phys. 8:6823–6838.